

# The Effects of Charged Charm Mesons on the Line Shapes of the $X(3872)$

Eric Braaten and Meng Lu

*Physics Department, Ohio State University, Columbus, Ohio 43210, USA*

(Dated: February 9, 2022)

## Abstract

The quantum numbers  $J^{PC} = 1^{++}$  of the  $X(3872)$  and the proximity of its mass to the  $D^{*0}\bar{D}^0$  threshold imply that it is either a loosely-bound hadronic molecule whose constituents are a superposition of  $D^{*0}\bar{D}^0$  and  $D^0\bar{D}^{*0}$  or it is a virtual state of charm mesons. The line shapes of the  $X(3872)$  can discriminate between these two possibilities. At energies within a few MeV of the  $D^{*0}\bar{D}^0$  threshold, the line shapes of the  $X$  produced in  $B \rightarrow K$  transitions are determined by its binding energy and its width. Their normalizations are determined by a short-distance constant that is different for  $B^+ \rightarrow K^+$  and  $B^0 \rightarrow K^0$ . At energies comparable to the 8 MeV splitting between the  $D^{*0}\bar{D}^0$  and  $D^{*+}D^-$  thresholds, the charged meson channels  $D^{*+}D^-$  and  $D^+D^{*-}$  have a significant effect on the line shapes of the  $X$ . We calculate the line shapes taking into account the resonant coupling between the charged and neutral  $1^{++}$  channels. The line shapes and their normalizations depend on one additional scattering parameter and two additional short-distance constants associated with the  $B \rightarrow K$  transitions. The line shapes of the  $X$  resonance depend on its decay channel; they are different for  $J/\psi \pi^+\pi^-$ ,  $J/\psi \pi^+\pi^-\pi^0$ , and  $D^0\bar{D}^0\pi^0$ . The line shapes are also different for  $X$  produced in  $B^+$  decays and in  $B^0$  decays. Some conceptual errors in previous work on this problem are pointed out.

PACS numbers: 12.38.-t, 12.39.St, 13.20.Gd, 14.40.Gx

## I. INTRODUCTION

The  $X(3872)$  is a  $c\bar{c}$  resonance near 3872 MeV discovered in 2003 by the Belle Collaboration [1] and subsequently observed by the CDF, Babar, and D0 Collaborations [2–4]. In addition to the discovery decay mode  $J/\psi \pi^+ \pi^-$ , the  $X$  has been observed to decay into  $J/\psi \gamma$ ,  $J/\psi \pi^+ \pi^- \pi^0$ , [5] and  $D^0 \bar{D}^0 \pi^0$  [6, 7]. The decay into  $J/\psi \gamma$  implies that the  $X$  is even under charge conjugation. An analysis by the Belle Collaboration of the decays of  $X$  into  $J/\psi \pi^+ \pi^-$  strongly favors the quantum numbers  $J^{PC} = 1^{++}$ , but does not exclude  $2^{++}$  [8]. An analysis by the CDF Collaboration of the decays of  $X$  into  $J/\psi \pi^+ \pi^-$  is compatible with the Belle constraints [9]. The tiny phase space available for the decay into  $D^0 \bar{D}^0 \pi^0$  rules out  $J = 2$ , leaving  $1^{++}$  as the only option.

An important feature of the  $X(3872)$  is that its mass  $M_X$  is extremely close to the  $D^{*0} \bar{D}^0$  threshold. The PDG value for  $M_X$  comes from combining measurements of  $X$  in the  $J/\psi \pi^+ \pi^-$  decay mode [10]. After taking into account a recent precision measurement of the  $D^0$  mass by the CLEO Collaboration [11], the difference between the PDG value for  $M_X$  and the  $D^{*0} \bar{D}^0$  threshold is

$$M_X - (M_{*0} + M_0) = -0.6 \pm 0.6 \text{ MeV}, \quad (1)$$

where  $M_{*0}$  and  $M_0$  are the masses of  $D^{*0}$  and  $D^0$ . The negative central value in Eq. (1) is compatible with the  $X$  being a bound state of the charm mesons. The measured mass of the near-threshold enhancement in  $D^0 \bar{D}^0 \pi^0$  is about 4 MeV above the  $D^{*0} \bar{D}^0$  threshold [6, 7]. This value is compatible with  $X$  being a virtual state of charm mesons. It differs from the mass in Eq. (1) by more than two standard deviations, which raises the question of whether the decays into  $J/\psi \pi^+ \pi^-$  and  $D^0 \bar{D}^0 \pi^0$  are coming from the same resonance.

The proximity of the mass of the  $X(3872)$  to the  $D^{*0} \bar{D}^0$  threshold has motivated its identification as a weakly-bound molecule whose constituents are a superposition of the charm meson pairs  $D^{*0} \bar{D}^0$  and  $D^0 \bar{D}^{*0}$  [12–15]. The establishment of the quantum numbers of the  $X(3872)$  as  $1^{++}$  makes this conclusion almost unavoidable. The reason is that these quantum numbers allow S-wave couplings of the  $X$  to  $D^{*0} \bar{D}^0$  and  $D^0 \bar{D}^{*0}$ . Nonrelativistic quantum mechanics implies that a resonance in an S-wave channel near a 2-particle threshold has special universal features [16]. Because of the small energy gap between the resonance and the 2-particle threshold, there is a strong coupling between the resonance and the two particles. This strong coupling generates dynamically a large length scale that can be identified with the absolute value of the S-wave scattering length  $a$  of the two particles. Independent of the original mechanism for the resonance, the strong coupling transforms the resonance into a bound state just below the two-particle threshold if  $a > 0$  or into a virtual state just above the two-particle threshold if  $a < 0$ . If  $a > 0$ , the bound state has a molecular structure, with the particles having a large mean separation of order  $a$ .

To see that the universal features of an S-wave threshold resonance are relevant to the  $X(3872)$ , we need only note that its binding energy is small compared to the natural energy scale associated with pion exchange [17]:  $m_\pi^2/(2M_{*00}) \approx 10 \text{ MeV}$ , where  $M_{*00}$  is the reduced mass of the two constituents. The universal features of the  $X(3872)$  were first exploited by Voloshin to describe its decays into  $D^0 \bar{D}^0 \pi^0$  and  $D^0 \bar{D}^0 \gamma$ , which can proceed through decay of the constituent  $D^{*0}$  or  $\bar{D}^{*0}$  [15]. Universality has also been applied to the production process  $B \rightarrow KX$  [18, 19], to the line shapes of the  $X$  [20], and to decays of  $X$  into  $J/\psi$  and pions [21]. These applications rely on factorization formulas that separate the length scale  $a$  from all the shorter distance scales of QCD [20]. The factorization formulas can be derived using the operator product expansion for a low-energy effective field theory [22].

Other interpretations of the  $X(3872)$  besides a charm meson molecule or a charm meson virtual state have been proposed, including a P-wave charmonium state or a tetraquark state. (For a review, see Ref. [23].) If the charmonium or tetraquark models were extended to include the coupling of the  $X$  to  $D^{*0}\bar{D}^0$  and  $D^0\bar{D}^{*0}$  scattering states, the universal features of an S-wave threshold resonance imply that the tuning of the binding energy to the threshold region would transform the state into a charm meson molecule or a virtual state of charm mesons. Any model of the  $X(3872)$  that does not take into account its strong coupling to charm meson scattering states should not be taken seriously.

Given that the quantum numbers of the  $X(3872)$  are  $1^{++}$ , the measured mass  $M_X$  in Eq. (1) implies unambiguously that  $X$  must be either a charm meson molecule or a virtual state of charm mesons. The remaining challenge is to discriminate between these two possibilities. If the  $X$  was sufficiently narrow, there would be clear qualitative differences in its line shapes between these two possibilities. We first consider the  $D^0\bar{D}^0\pi^0$  decay mode, which has a contribution from the decay of a constituent  $D^{*0}$ . If the  $X$  was a charm meson molecule, its line shape in  $D^0\bar{D}^0\pi^0$  would consist of a Breit-Wigner resonance below the  $D^{*0}\bar{D}^0$  threshold and a threshold enhancement above the  $D^{*0}\bar{D}^0$  threshold. If the  $X$  was a virtual state, there would only be the threshold enhancement above the  $D^{*0}\bar{D}^0$  threshold. We next consider decay modes that have no contributions from the decay of a constituent  $D^{*0}$ , such as  $J/\psi\pi^+\pi^-$ . If the  $X$  was a charm meson molecule, its line shape in such a decay mode would be a Breit-Wigner resonance below the  $D^{*0}\bar{D}^0$  threshold. If the  $X$  was a virtual state, there would only be a cusp at the  $D^{*0}\bar{D}^0$  threshold. The possibility of interpreting the  $X(3872)$  as a cusp at the  $D^{*0}\bar{D}^0$  threshold has been suggested by Bugg [24]. Increasing the width of the  $X$  provides additional smearing of the line shapes. This makes the qualitative difference between the line shapes of a charm meson molecule and a virtual state less dramatic. To discriminate between these two possibilities therefore requires a quantitative analysis.

There have been two recent analyses of data on  $B \rightarrow K + X$  that shed light on the issue of whether the  $X$  is a bound state or a virtual state. Hanhart et al. [25] analyzed the data on  $B^+ \rightarrow K^+ + J/\psi\pi^+\pi^-$  and  $B^+ \rightarrow K^+ + D^0\bar{D}^0\pi^0$  from the Belle and Babar Collaborations using a model for the scattering amplitude in the  $D^{*0}\bar{D}^0 + D^0\bar{D}^{*0}$  channel that is a generalization of the Flatté parametrization for a near-threshold resonance. They concluded that the  $D^0\bar{D}^0\pi^0$  threshold enhancement observed by the Belle and Babar Collaborations is compatible with the  $X(3872)$  only if the  $X$  is a virtual state. One flaw in the analysis of Ref. [25] is that it did not take into account the width of the constituent  $D^{*0}$ . They also assumed incorrectly that a bound state below the  $D^{*0}\bar{D}^0$  threshold would not decay into  $D^0\bar{D}^0\pi^0$ .

In Ref. [26], we derived the line shapes of the  $X(3872)$  near the  $D^{*0}\bar{D}^0$  threshold from the assumption of an S-wave resonance in the neutral charm meson channel  $D^{*0}\bar{D}^0 + D^0\bar{D}^{*0}$ . We developed expressions for the line shapes that take into account the width of the  $D^{*0}$  meson and the inelastic scattering channels of the charm mesons. An analysis of the data on  $B^+ \rightarrow K^+ + J/\psi\pi^+\pi^-$  and  $B^+ \rightarrow K^+ + D^0\bar{D}^0\pi^0$  from the Belle Collaboration indicated that the data preferred the  $X(3872)$  to be a bound state but a virtual state was not excluded. The most important lesson of the analyses of Refs. [25] and [26] is that the measured difference between the masses of the  $X(3872)$  in the  $J/\psi\pi^+\pi^-$  and  $D^0\bar{D}^0\pi^0$  decay channels is consistent with it being a charm meson molecule or a virtual state of charm mesons.

In this paper, we generalize the results of Ref. [26] for the line shapes of the  $X(3872)$  to take into account the resonant coupling between the neutral charm meson channel and the

charged charm meson channel  $D^{*+}D^- + D^+D^{*-}$ . In Sec. II, we summarize the results of Ref. [26] for the energy-dependent widths of virtual  $D^*$  mesons. In Ref. [26], we developed an expression for the resonant scattering amplitude for the neutral charm meson channel that takes into account the  $D^{*0}$  width and inelastic charm meson scattering channels. In Sec. III, we extend that result to the three scattering amplitudes for the resonantly coupled neutral and charged charm meson channels. In Ref. [26], we derived factorization formulas for the line shapes of  $X(3872)$  in the decays  $B \rightarrow K + X$  that take into account the resonance in the neutral charm meson channel. In Section IV, we extend those results to take into account the resonant coupling to the charged charm meson channel. In Sec. V, we summarize our results.

## II. MASSES AND $D^*$ WIDTHS

When we consider the decays of the  $D^*$  mesons, there are particles with six different masses that must be considered. We therefore introduce concise notation for the masses of the charm mesons and the pions. We denote the masses of the spin-0 charm mesons  $D^0$  and  $D^+$  by  $M_0$  and  $M_1$ , respectively. We denote the masses of the spin-1 charm mesons  $D^{*0}$  and  $D^{*+}$  by  $M_{*0}$  and  $M_{*1}$ , respectively. We denote the masses of the pions  $\pi^0$  and  $\pi^+$  by  $m_0$  and  $m_1$ , respectively. (The numerical subscript is the absolute value of the electric charge of the meson.) The pion mass scale corresponding to either  $m_0$  or  $m_1$  will be denoted by  $m_\pi$ . The result of a recent precision measurement of the  $D^0$  mass by the CLEO Collaboration is  $M_0 = 1864.85 \pm 0.18$  MeV, where we have combined the errors in quadrature [11]. We use the PDG values for the other masses [10]. The errors on the pion masses are negligible compared to those on the charm meson masses. Some of the differences between the charm meson masses have errors that are significantly smaller than the errors in the masses themselves.

We also introduce concise notations for simple combinations of the masses. We denote the reduced mass of a spin-1 charm meson and a spin-0 charm meson by

$$M_{*ij} = \frac{M_{*i}M_j}{M_{*i} + M_j}. \quad (2)$$

We denote the reduced mass of a pion and a spin-0 charm meson by

$$m_{ij} = \frac{m_iM_j}{m_i + M_j}. \quad (3)$$

We denote the differences between the  $D^*$  masses and  $D\pi$  thresholds by

$$\delta_{ijk} = M_{*i} - M_j - m_k. \quad (4)$$

The differences between the  $D^*$  masses and the thresholds for  $D\pi$  states with the same electric charge are

$$\delta_{000} = 7.14 \pm 0.07 \text{ MeV}, \quad (5a)$$

$$\delta_{011} = -2.23 \pm 0.12 \text{ MeV}, \quad (5b)$$

$$\delta_{101} = 5.85 \pm 0.01 \text{ MeV}, \quad (5c)$$

$$\delta_{110} = 5.66 \pm 0.10 \text{ MeV}. \quad (5d)$$

The isospin splittings between the charm meson masses are  $M_1 - M_0 \approx 4.8$  MeV and  $M_{*1} - M_{*0} \approx 3.3$  MeV. The energy splitting  $\nu = (M_{*1} + M_1) - (M_{*0} + M_0)$  between the  $D^{*+}D^-$  and  $D^{*0}\bar{D}^0$  thresholds is

$$\nu = 8.08 \pm 0.12 \text{ MeV}. \quad (6)$$

A phenomenological analysis of the decays of the  $D^{*0}$  and  $D^{*+}$  was presented in Ref. [26]. We summarize here the results of that analysis, which was based on chiral symmetry and isospin symmetry. The PDG value for the total width of the  $D^{*+}$  is  $\Gamma[D^{*+}] = 96 \pm 22$  keV [10]. Using the PDG values for the branching fractions for  $D^{*+}$  decays, we obtain measured values for the partial widths for  $D^{*+}$  decays:

$$\Gamma[D^{*+} \rightarrow D^0\pi^+] = 65.0 \pm 14.9 \text{ keV}, \quad (7a)$$

$$\Gamma[D^{*+} \rightarrow D^+\pi^0] = 29.5 \pm 6.8 \text{ keV}, \quad (7b)$$

$$\Gamma[D^{*+} \rightarrow D^+\gamma] = 1.5 \pm 0.5 \text{ keV}. \quad (7c)$$

Using isospin symmetry and the PDG values for the branching fractions for  $D^{*0}$  decays, we obtain predictions for the partial widths for  $D^{*0}$  decays:

$$\Gamma[D^{*0} \rightarrow D^0\pi^0] = 40.5 \pm 9.3 \text{ keV}, \quad (8a)$$

$$\Gamma[D^{*0} \rightarrow D^0\gamma] = 25.0 \pm 6.2 \text{ keV}. \quad (8b)$$

The prediction for the total width of the  $D^{*0}$  is  $\Gamma[D^{*0}] = 65.5 \pm 15.4$  keV.

The decay rates for  $D^* \rightarrow D\pi$  are fairly sensitive to the mass of the  $D^*$ , since they scale like the 3/2 power of the energy difference between the  $D^*$  mass and the  $D\pi$  threshold. A virtual  $D^{*0}$  (or  $D^{*+}$ ) with energy  $M_{*0} + E$  (or  $M_{*1} + E$ ) can be considered as a  $D^*$  whose rest energy differs from its physical mass by the energy  $E$ . The width of the virtual particle varies with  $E$ . We denote the energy-dependent widths of the  $D^{*+}$  and  $D^{*0}$  by  $\Gamma_{*1}(E)$  and  $\Gamma_{*0}(E)$ , respectively. If  $|E|$  is small compared to  $m_\pi$ , these energy-dependent widths can be obtained simply by scaling the physical partial widths for the decays  $D^* \rightarrow D\pi$ :

$$\begin{aligned} \Gamma_{*0}(E) = & \Gamma[D^{*0} \rightarrow D^0\gamma] + \Gamma[D^{*0} \rightarrow D^0\pi^0] \left[ [(\delta_{000} + E)/\delta_{000}]^{3/2} \theta(\delta_{000} + E) \right. \\ & \left. + 2(m_{11}/m_{00})^{5/2} [(\delta_{011} + E)/\delta_{000}]^{3/2} \theta(\delta_{011} + E) \right], \end{aligned} \quad (9a)$$

$$\begin{aligned} \Gamma_{*1}(E) = & \Gamma[D^{*+} \rightarrow D^+\gamma] + \Gamma[D^{*+} \rightarrow D^+\pi^0] [(\delta_{110} + E)/\delta_{110}]^{3/2} \theta(\delta_{110} + E) \\ & + \Gamma[D^{*+} \rightarrow D^0\pi^+] [(\delta_{101} + E)/\delta_{101}]^{3/2} \theta(\delta_{101} + E). \end{aligned} \quad (9b)$$

We ignore any energy dependence of the decay widths into  $D\gamma$ , because the photon energy and the phase space for the decays  $D^* \rightarrow D\gamma$  do not vary significantly in the  $D^*\bar{D}$  threshold region. In Fig. 1, we plot the energy-dependent widths  $\Gamma_{*0}(E)$  and  $\Gamma_{*1}(E - \nu)$  as functions of  $E$ . The offset  $\nu \approx 8.1$  MeV in  $\Gamma_{*1}(E - \nu)$  was chosen so that  $\Gamma_{*0}(E)$  and  $\Gamma_{*1}(E - \nu)$  are the relevant widths for a  $D^*\bar{D}$  system consisting of  $\bar{D}$  and a  $D^*$  with total energy  $E$  relative to the  $D^{*0}\bar{D}^0$  threshold. Thus  $\Gamma_{*0}(E)$  reduces to  $\Gamma[D^{*0}]$  at  $E = 0$  and  $\Gamma_{*1}(E - \nu)$  reduces to  $\Gamma[D^{*+}]$  at  $E = \nu$ . The physical widths  $\Gamma[D^{*0}]$  and  $\Gamma[D^{*+}]$  are shown in Fig. 1 as data points with error bars. At the  $D^{*0}\bar{D}^0$  threshold, the energy-dependent width of the  $D^{*+}$  is  $\Gamma_{*1}(-\nu) \approx 1.5$  MeV.

The individual terms in Eqs. (9) have obvious interpretations as energy-dependent partial widths for decays of  $D^{*+}$  and  $D^{*0}$ . We can define energy-dependent branching fractions by

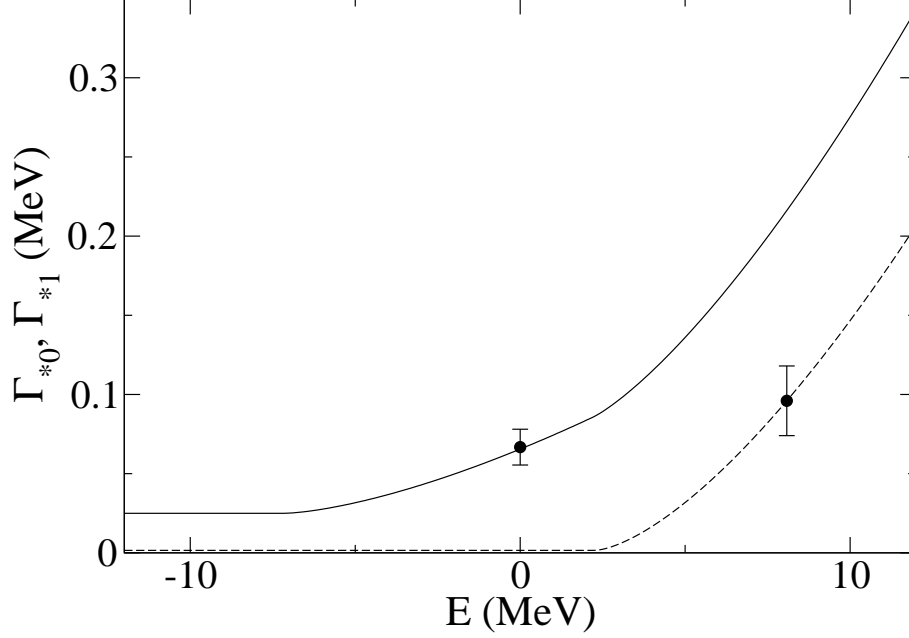


FIG. 1: The energy-dependent widths  $\Gamma_{*0}(E)$  and  $\Gamma_{*1}(E-\nu)$  for a virtual  $D^{*0}$  with energy  $M_{*0} + E$  and a virtual  $D^{*+}$  with energy  $M_{*1} + E - \nu$ , respectively, as functions of  $E$ . The points with error bars at  $E = 0$  and  $E = \nu$  indicate the central values and uncertainties of the physical widths of  $D^{*0}$  and  $D^{*+}$ , respectively.

dividing these terms by  $\Gamma_{*1}(E)$  or  $\Gamma_{*0}(E)$ . For example, the energy-dependent branching fractions for  $D^{*0} \rightarrow D^0 \pi^0$  and  $D^{*+} \rightarrow D^+ \pi^0$  are

$$\text{Br}_{000}(E) = \frac{\Gamma[D^{*0} \rightarrow D^0 \pi^0]}{\Gamma_{*0}(E)} [(\delta_{000} + E)/\delta_{000}]^{3/2} \theta(\delta_{000} + E), \quad (10a)$$

$$\text{Br}_{110}(E) = \frac{\Gamma[D^{*+} \rightarrow D^+ \pi^0]}{\Gamma_{*1}(E)} [(\delta_{110} + E)/\delta_{110}]^{3/2} \theta(\delta_{110} + E). \quad (10b)$$

The standard isospin multiplets for the charm mesons are  $(-D^+, D^0)$ ,  $(\bar{D}^0, D^-)$ ,  $(-D^{*+}, D^{*0})$ , and  $(\bar{D}^{*0}, D^{*-})$ , where the first and second states are the upper and lower components of the multiplet, respectively. The  $D^* \bar{D}$  channels with charge conjugation quantum number  $C = +$  are

$$(D^* \bar{D})_+^0 = +\frac{1}{\sqrt{2}} (D^{*0} \bar{D}^0 + D^0 \bar{D}^{*0}), \quad (11a)$$

$$(D^* \bar{D})_+^1 = -\frac{1}{\sqrt{2}} (D^{*+} D^- + D^+ D^{*-}). \quad (11b)$$

The superscript  $i$  on  $(D^* \bar{D})_+^i$  is the absolute value of the electric charge of either meson. We will refer to  $(D^* \bar{D})_+^0$  and  $(D^* \bar{D})_+^1$  as the neutral and charged charm meson channels, respectively. The channels with isospin quantum numbers  $I = 0$  and  $I = 1$  are the antisymmetric and symmetric linear combinations of these neutral and charged channels, respectively:

$$(D^* \bar{D})_+^{I=0} = \frac{1}{\sqrt{2}} [(D^* \bar{D})_+^0 - (D^* \bar{D})_+^1], \quad (12a)$$

$$(D^* \bar{D})_+^{I=1} = \frac{1}{\sqrt{2}} [(D^* \bar{D})_+^0 + (D^* \bar{D})_+^1]. \quad (12b)$$

### III. LOW-ENERGY $D^*\bar{D}$ SCATTERING

In this section, we discuss the low-energy scattering of charm mesons. We first summarize the results of Ref. [26], which took into account only the neutral channel  $(D^*\bar{D})_+^0$ . These results should be accurate when the energy  $E$  is within a few MeV of the  $D^{*0}\bar{D}^0$  threshold. We then extend the region of validity to the entire  $D^*\bar{D}$  threshold region by taking into account the resonant coupling to the charged channel  $(D^*\bar{D})_+^1$ .

#### A. Neutral channel only

We begin by writing down a general expression for the transition amplitude for S-wave scattering in the  $(D^*\bar{D})_+^0$  channel that is compatible with unitarity. The transition amplitude  $\mathcal{A}(E)$  for the scattering of nonrelativistically normalized charm mesons in the channel  $(D^*\bar{D})_+^0$  can be written in the form

$$\mathcal{A}(E) = \frac{2\pi}{M_{*00}} f(E), \quad (13)$$

where  $f(E)$  is the conventional nonrelativistic scattering amplitude expressed as a function of the total energy of the charm mesons. An expression for the scattering amplitude that is compatible with unitarity is

$$f(E) = \frac{1}{-\gamma + \kappa(E)}, \quad (14)$$

where  $\kappa(E) = (-2M_{*00}E - i\varepsilon)^{1/2}$  and  $E$  is the total energy relative to the  $D^{*0}\bar{D}^0$  threshold in the center-of-mass frame. If the inverse scattering length  $\gamma$  is complex, the imaginary part of the scattering amplitude in Eq. (14) is

$$\text{Im } f(E) = |f(E)|^2 \text{Im } [\gamma - \kappa(E)]. \quad (15)$$

The scattering amplitude  $f(E)$  in Eq. (14) satisfies the constraints of unitarity for a single-channel system exactly provided  $\gamma$  is a real function of  $E$ . For positive real values of the energy  $E$ , Eq. (15) is simply the optical theorem for this single-channel system:

$$\text{Im } f(E) = |f(E)|^2 \sqrt{2M_{*00}E} \quad (E > 0). \quad (16)$$

The left side is the imaginary part of the T-matrix element for elastic scattering in the  $(D^*\bar{D})_+^0$  channel multiplied by  $M_{*00}/(2\pi)$ . The right side is the cross section for elastic scattering multiplied by  $(2M_{*00}E)^{1/2}/(4\pi)$ . We first consider the case  $\gamma > 0$ . In this case, the amplitude  $f(E)$  has a pole at a negative value of the energy  $E$ , indicating the existence of a stable bound state. If  $\gamma$  varies sufficiently slowly with  $E$  that it can be approximated by a constant, the pole is near  $E_{\text{pole}} \approx -\gamma^2/(2M_{*00})$  and the binding energy is  $\gamma^2/(2M_{*00})$ . In addition to the contribution to the imaginary part of  $f(E)$  in Eq. (16), there is a delta-function contribution at  $E = E_{\text{pole}}$ :

$$\text{Im } f(E) \approx \frac{\pi\gamma}{M_{*00}} \delta(E + \gamma^2/(2M_{*00})) \quad (E < 0, \gamma > 0). \quad (17)$$

We next consider the case  $\gamma < 0$ . In this case, the pole in the amplitude  $f(E)$  is not on the real  $E$  axis, but on the second sheet of the complex variable  $E$ . The standard terminology

for such a pole is a *virtual state*. The imaginary part of the amplitude is nonzero only in the positive  $E$  region and is given by Eq. (16).

Scattering in the  $(D^*\bar{D})_+^0$  channel cannot be exactly unitary, because the  $D^{*0}$  has a nonzero width and because the charm mesons have inelastic scattering channels. The inelastic channels include  $D^0\bar{D}^0\pi^0$  and  $D^0\bar{D}^0\gamma$ , which are related to  $D^{*0}$  or  $\bar{D}^{*0}$  decays, as well as all other decay modes of  $X(3872)$ , including  $J/\psi\pi^+\pi^-$ ,  $J/\psi\pi^+\pi^-\pi^0$ , and  $J/\psi\gamma$ . In Ref. [26], the dominant effects of the  $D^{*0}$  width and the inelastic scattering channels were taken into account through simple modifications of the variables  $\gamma$  and  $\kappa(E)$  in the scattering amplitude  $f(E)$  in Eq. (14). The effects of the decays of the constituent  $D^{*0}$  or  $\bar{D}^{*0}$  were taken into account simply by replacing the mass  $M_{*0}$  that is implicit in the energy  $E$  measured from the  $D^{*0}\bar{D}^0$  threshold by  $M_{*0} - i\Gamma_{*0}(E)/2$ , where  $\Gamma_{*0}(E)$  is the energy-dependent width of the  $D^{*0}$  given in Eq. (9a). This changes the energy variable  $\kappa(E) = (-2M_{*0}E - i\varepsilon)^{1/2}$  into

$$\kappa(E) = \sqrt{-2M_{*0}[E + i\Gamma_{*0}(E)/2]}. \quad (18)$$

At the threshold  $E = 0$ , the energy-dependent width  $\Gamma_{*0}(E)$  reduces to the physical width  $\Gamma[D^{*0}]$ . The expression for  $\kappa(E)$  in Eq. (18) requires a choice of branch cut for the square root. If  $E$  is real, an explicit expression for  $\kappa(E)$  that corresponds to the appropriate choice of branch cut can be obtained by using the identity

$$\sqrt{-2M[E + i\Gamma/2]} = \sqrt{M} \left[ \left( \sqrt{E^2 + \Gamma^2/4} - E \right)^{1/2} - i \left( \sqrt{E^2 + \Gamma^2/4} + E \right)^{1/2} \right]. \quad (19)$$

In Ref. [26], the effects of inelastic scattering channels for the charm mesons other than  $D^0\bar{D}^0\pi^0$  and  $D^0\bar{D}^0\gamma$  were taken into account by replacing the real parameter  $\gamma$  by a complex parameter with a positive imaginary part. The expression for the imaginary part of the amplitude  $f(E)$  in Eq. (15) can now be interpreted as the optical theorem for a multi-channel system consisting of  $(D^*\bar{D})_+^0$  and all the inelastic scattering channels. The right side can be interpreted as the total cross section for scattering in the  $(D^*\bar{D})_+^0$  channel multiplied by  $(2M_{*0}E)^{1/2}/(4\pi)$ . The terms proportional to  $\text{Im}\kappa(E)$  and  $\text{Im}\gamma$  are proportional to the elastic and inelastic cross sections, respectively. This interpretation requires  $\text{Im}\gamma > 0$ .

The scattering amplitude  $f(E)$  in Eq. (14) with  $\kappa(E)$  given by Eq. (18) and a complex parameter  $\gamma$  has a pole at an energy  $E_{\text{pole}}$  that is not on the real axis. If the difference between  $\Gamma_{*0}(E_{\text{pole}})$  and  $\Gamma_{*0}(0)$  is small compared to  $\Gamma[D^{*0}]$ , the pole energy can be approximated by

$$E_{\text{pole}} \approx -\frac{\gamma^2}{2M_{*0}} - i\Gamma[D^{*0}]/2. \quad (20)$$

The energy  $E_{\text{pole}}$  is that of a bound state if  $\text{Re}\gamma > 0$  and that of a virtual state if  $\text{Re}\gamma < 0$ .

## B. Coupled neutral and charged channels

We now generalize the results of Section III A to the system consisting of the two coupled channels  $(D^*\bar{D})_+^0$  and  $(D^*\bar{D})_+^1$  defined by Eqs. (11). The amplitudes for transitions between these channels can be expressed as a  $2 \times 2$  matrix  $\mathcal{A}_{ij}(E)$ ,  $i, j \in \{0, 1\}$ . We first write down a general expression for the transition amplitudes for S-wave scattering in the two channels that is compatible with unitarity in this two-channel system. A convenient way to



parametrize these amplitudes is to express the inverse of the matrix of amplitudes  $\mathcal{A}_{ij}(E)$  in the form

$$\mathcal{A}(E)^{-1} = \frac{1}{2\pi} \begin{pmatrix} \sqrt{M_{*00}} & 0 \\ 0 & \sqrt{M_{*11}} \end{pmatrix} \begin{pmatrix} -\gamma_{00} + \kappa(E) & -\gamma_{01} \\ -\gamma_{01} & -\gamma_{11} + \kappa_1(E) \end{pmatrix} \begin{pmatrix} \sqrt{M_{*00}} & 0 \\ 0 & \sqrt{M_{*11}} \end{pmatrix}, \quad (21)$$

where  $\kappa(E) = (-2M_{*00}E - i\varepsilon)^{1/2}$ ,  $\kappa_1(E) = (-2M_{*11}(E - \nu) - i\varepsilon)^{1/2}$ , and  $E$  is the energy relative to the  $D^{*0}\bar{D}^0$  threshold. The parametrization of the inverse matrix in Eq. (21) was chosen so that the analytic expressions for the entries of  $\mathcal{A}_{ij}(E)$  would be as simple as possible. It is convenient to define a matrix  $f_{ij}(E)$  of scattering amplitudes by

$$\mathcal{A}_{ij}(E) = \frac{2\pi}{\sqrt{M_{*ii}M_{*jj}}} f_{ij}(E). \quad (22)$$

The entries of the matrix  $f_{ij}(E)$  are

$$f_{00}(E) = \left( -\gamma_{00} + \kappa(E) - \frac{\gamma_{01}^2}{-\gamma_{11} + \kappa_1(E)} \right)^{-1}, \quad (23a)$$

$$f_{01}(E) = \left( -\gamma_{01} + \frac{[-\gamma_{00} + \kappa(E)][-\gamma_{11} + \kappa_1(E)]}{\gamma_{01}} \right)^{-1}, \quad (23b)$$

$$f_{11}(E) = \left( -\gamma_{11} + \kappa_1(E) - \frac{\gamma_{01}^2}{-\gamma_{00} + \kappa(E)} \right)^{-1}. \quad (23c)$$

If the parameters  $\gamma_{00}$ ,  $\gamma_{01}$ , and  $\gamma_{11}$  are complex, the imaginary parts of the scattering amplitudes in Eq. (23) satisfy

$$\begin{aligned} \text{Im } f_{ij}(E) &= f_{i0}(E) f_{j0}^*(E) \text{Im} [\gamma_{00} - \kappa(E)] + f_{i1}(E) f_{j1}^*(E) \text{Im} [\gamma_{11} - \kappa_1(E)] \\ &\quad + (f_{i0}(E) f_{j1}^*(E) + f_{i1}(E) f_{j0}^*(E)) \text{Im} [\gamma_{01}]. \end{aligned} \quad (24)$$

Since  $\text{Im } f_{ij}(E)$  is real, an alternative form for this unitarity equation can be obtained by taking the complex conjugate of the right side.

The amplitudes  $f_{ij}(E)$  in Eqs. (23) satisfy the constraints of unitarity for this two-channel system exactly if  $\gamma_{00}$ ,  $\gamma_{01}$ , and  $\gamma_{11}$  are all real functions of  $E$ . For positive real values of the energy  $E$ , the expressions in Eqs. (24) for the imaginary parts of the amplitudes  $f_{00}(E)$  and  $f_{11}(E)$  are just the optical theorems for this two-channel system:

$$\text{Im } f_{00}(E) = |f_{00}(E)|^2 \sqrt{2M_{*00}E} + |f_{01}(E)|^2 \sqrt{2M_{*11}(E - \nu)} \theta(E - \nu), \quad (25a)$$

$$\text{Im } f_{11}(E) = |f_{01}(E)|^2 \sqrt{2M_{*00}E} + |f_{11}(E)|^2 \sqrt{2M_{*11}(E - \nu)} \theta(E - \nu). \quad (25b)$$

The left sides of Eqs. (25a) and (25b) are proportional to the imaginary parts of the T-matrix elements for elastic scattering in the  $(D^*\bar{D})_+^0$  and  $(D^*\bar{D})_+^1$  channels, respectively. The first and second terms on the right side of each equation are proportional to the cross sections for scattering into the  $(D^*\bar{D})_+^0$  and  $(D^*\bar{D})_+^1$  channels, respectively. In the region  $E < 0$ , the imaginary parts of  $f_{00}(E)$  and  $f_{11}(E)$  may also have delta function contributions analogous to the one in Eq. (17).

There are two limits in which the amplitudes  $f_{01}(E)$  and  $f_{11}(E)$  go to 0 and  $f_{00}(E)$  reduces to the single-channel amplitude in Eq. (14). The first limit is  $\nu \rightarrow +\infty$ , which

corresponds to increasing the energy gap between the two thresholds. In this case,  $f_{00}(E)$  reduces to Eq. (14) with  $\gamma = \gamma_{00}$ . The second limit is  $\gamma_{01}, \gamma_{11} \rightarrow \infty$  with  $\gamma_{01}^2/\gamma_{11}$  fixed, which corresponds to decreasing the interaction strength between the two channels. In this case,  $f_{00}(E)$  again reduces to Eq. (14) but with  $\gamma = \gamma_{00} - \gamma_{01}^2/\gamma_{11}$ .

Scattering in the  $(D^*\bar{D})_+^0$  and  $(D^*\bar{D})_+^1$  channels cannot be exactly unitary, because the  $D^{*0}$  and  $D^{*+}$  have nonzero widths and because the charm mesons have inelastic scattering channels. The inelastic channels include  $D\bar{D}\pi$  and  $D\bar{D}\gamma$ , which are related to  $D^*$  or  $\bar{D}^*$  decays, as well as all the decay modes of  $X(3872)$ , which include  $J/\psi \pi^+\pi^-$ ,  $J/\psi \pi^+\pi^-\pi^0$ , and  $J/\psi \gamma$ . The effects of decays of  $D^{*0}$  and  $\bar{D}^{*0}$  can be taken into account by replacing  $\kappa(E)$  in the amplitudes in Eqs. (23) by the expression in Eq. (18). Similarly the effects of decays of  $D^{*+}$  and  $D^{*-}$  can be taken into account by replacing  $\kappa_1(E)$  in the amplitudes in Eqs. (23) by

$$\kappa_1(E) = \sqrt{-2M_{*11}[E - \nu + i\Gamma_{*1}(E - \nu)/2]}. \quad (26)$$

At the  $D^{*+}D^-$  threshold  $E = \nu$ , the energy-dependent width  $\Gamma_{*1}(E - \nu)$  reduces to the physical width  $\Gamma[D^{*+}]$ . If  $E$  is real, an explicit expression for  $\kappa_1(E)$  that corresponds to the appropriate choice of the square-root branch cut in Eq. (26) can be obtained by using the identity in Eq. (19). The effects of inelastic scattering channels other than  $D\bar{D}\pi$  and  $D\bar{D}\gamma$  can be taken into account by replacing the real parameters  $\gamma_{00}$ ,  $\gamma_{01}$ , and  $\gamma_{11}$  by complex parameters with positive imaginary parts. The expression in Eq. (24) for the imaginary part of the amplitude  $f_{ii}(E)$  can now be interpreted as the optical theorem for the multi-channel system consisting of  $(D^*\bar{D})_+^0$ ,  $(D^*\bar{D})_+^1$ , and all the inelastic scattering channels. The right side can be interpreted as the total cross section for scattering in the  $(D^*\bar{D})_+^i$  channel multiplied by  $(2M_{*ii}E)^{1/2}/(4\pi)$ . The terms proportional to  $\text{Im}\kappa(E)$  and  $\text{Im}\kappa_1(E)$  are the cross sections for scattering into the  $(D^*\bar{D})_+^0$  and  $(D^*\bar{D})_+^1$  channels. The terms proportional to  $\text{Im}\gamma_{00}$ ,  $\text{Im}\gamma_{01}$ , and  $\text{Im}\gamma_{11}$  give the remaining inelastic cross sections. This interpretation requires  $\text{Im}\gamma_{00} > 0$  and  $\text{Im}\gamma_{11} > 0$ .

### C. Constraints from isospin symmetry

We now proceed to exploit the approximate isospin symmetry of QCD. Deviations from isospin symmetry can be treated as small perturbations except at low energies that are comparable to the isospin splittings between hadron masses, which in the case of charm hadrons are less than 5 MeV. In strong interaction processes, isospin-symmetry-violating effects come primarily from hadron mass differences. Exact isospin symmetry would require the masses of the charged charm mesons to be equal to those of their neutral counterparts, which implies  $\nu = 0$  and  $M_{*11} = M_{*00}$ . It would also require the inverse matrix of amplitudes in Eq. (21) to be diagonal in the isospin basis. These conditions can be expressed as

$$U \begin{pmatrix} -\gamma_{00} + \kappa(E) & -\gamma_{01} \\ -\gamma_{01} & -\gamma_{11} + \kappa(E) \end{pmatrix} U^\dagger = \begin{pmatrix} -\gamma_0 + \kappa(E) & 0 \\ 0 & -\gamma_1 + \kappa(E) \end{pmatrix}, \quad (27)$$

where  $\gamma_0$  and  $\gamma_1$  are the inverse scattering lengths in the isospin-symmetry limit for the  $I = 0$  and  $I = 1$  channels, respectively, and  $U$  is the unitary matrix associated with the transformation between the charged/neutral basis in Eqs. (11) and the isospin basis in

Eqs. (12). The conditions in Eq. (27) imply

$$\gamma_{00} = (\gamma_1 + \gamma_0)/2, \quad (28a)$$

$$\gamma_{01} = (\gamma_1 - \gamma_0)/2, \quad (28b)$$

$$\gamma_{11} = (\gamma_1 + \gamma_0)/2. \quad (28c)$$

The constraints on the amplitudes  $f_{ij}(E)$  from the approximate isospin symmetry of QCD are obtained by inserting these values for the parameters into Eqs. (23).

In terms of the parameters  $\gamma_0$  and  $\gamma_1$ , the scattering amplitudes in Eqs. (23) reduce to

$$f_{00}(E) = \frac{-(\gamma_0 + \gamma_1) + 2\kappa_1(E)}{D(E)}, \quad (29a)$$

$$f_{01}(E) = \frac{\gamma_1 - \gamma_0}{D(E)}, \quad (29b)$$

$$f_{11}(E) = \frac{-(\gamma_0 + \gamma_1) + 2\kappa(E)}{D(E)}, \quad (29c)$$

where the denominator is

$$D(E) = 2\gamma_1\gamma_0 - (\gamma_1 + \gamma_0)[\kappa(E) + \kappa_1(E)] + 2\kappa_1(E)\kappa(E). \quad (30)$$

The unitarity conditions in Eq. (24) can be written

$$\begin{aligned} \text{Im } f_{ij}(E) = & f_{i0}(E) f_{j0}^*(E) \text{Im} [\gamma_1 + \gamma_0 - 2\kappa(E)] / 2 \\ & + f_{i1}(E) f_{j1}^*(E) \text{Im} [\gamma_1 + \gamma_0 - 2\kappa_1(E)] / 2 \\ & + (f_{i0}(E) f_{j1}^*(E) + f_{i1}(E) f_{j0}^*(E)) \text{Im} [\gamma_1 - \gamma_0] / 2. \end{aligned} \quad (31)$$

If there is a bound state or virtual state near the  $D^{*0}\bar{D}^0$  threshold with complex energy  $E_{\text{pole}}$ , the denominator  $D(E)$  given in Eq. (30) vanishes at that energy. If we define a variable  $\gamma$  by

$$\gamma = \kappa(E_{\text{pole}}), \quad (32)$$

the equation  $D(E_{\text{pole}}) = 0$  can be expressed as

$$\gamma\kappa_1(E_{\text{pole}}) - \frac{1}{2}(\gamma_1 + \gamma_0)[\gamma + \kappa_1(E_{\text{pole}})] + \gamma_1\gamma_0 = 0. \quad (33)$$

The variable  $\gamma$  can be identified with the inverse scattering length introduced in Eq. (14). The energy  $E_{\text{pole}}$  is given approximately by Eq. (20). If we neglect the small difference between  $\kappa_1(E_{\text{pole}})$  and  $\kappa_1(0)$ , one can obtain an approximate solution of Eq. (33) for  $\gamma_0$  in terms of  $\gamma_1$  and  $\gamma$ :

$$\gamma_0 \approx \frac{\gamma_1\kappa_1(0) + \gamma_1\gamma - 2\kappa_1(0)\gamma}{2\gamma_1 - \kappa_1(0) - \gamma}. \quad (34)$$

If the energy  $E$  is within a few MeV of the  $D^{*0}\bar{D}^0$  threshold, the scattering amplitudes in Eqs. (29) can be simplified. If the small difference between  $\kappa_1(E)$  and  $\kappa_1(0)$  is neglected, the denominator  $D(E)$  given in Eq. (30) reduces to

$$D(E) \approx -[\gamma_1 + \gamma_0 - 2\kappa_1(0)][-\gamma + \kappa(E)]. \quad (35)$$

In the numerators,  $\kappa(E)$  and  $\gamma$  can be neglected compared to  $\kappa_1(0)$ ,  $\gamma_0$ , and  $\gamma_1$ . The scattering amplitudes then reduce to

$$f_{00}(E) \approx f(E), \quad (36a)$$

$$f_{10}(E) \approx \frac{\gamma_0 - \gamma_1}{\gamma_1 + \gamma_0 - 2\kappa_1(0)} f(E), \quad (36b)$$

$$f_{11}(E) \approx \frac{\gamma_1 + \gamma_0}{\gamma_1 + \gamma_0 - 2\kappa_1(0)} f(E), \quad (36c)$$

where  $f(E)$  is the single-channel scattering amplitude in Eq. (14). If  $\gamma$  is neglected compared to  $\kappa_1(0)$  and  $\gamma_1$ , the expression for  $\gamma_0$  in Eq. (34) reduces to

$$\gamma_0 \approx \frac{\gamma_1 \kappa_1(0)}{2\gamma_1 - \kappa_1(0)}. \quad (37)$$

Using this expression to eliminate  $\gamma_0$  in favor of  $\gamma_1$ , the coefficient of  $f(E)$  in the amplitudes  $f_{ij}(E)$  in Eqs. (36) can be factored into a term that depends on the channel  $i$  and a term that depends on the channel  $j$ :

$$f_{ij}(E) \approx c_i f(E) c_j, \quad (38)$$

where the coefficients  $c_i$  are given by

$$c_0 = 1, \quad (39a)$$

$$c_1 = -\frac{\gamma_1}{\gamma_1 - \kappa_1(0)}. \quad (39b)$$

The values of the two independent parameters  $\gamma_0$  and  $\gamma_1$  could be calculated using potential models for heavy mesons with pion-exchange interactions. As pointed out by Tornqvist in 1993, these models indicate that there should be  $D^*\bar{D}$  bound states near threshold in several  $I = 0$  channels, including the S-wave  $1^{++}$  channel, but not in any of the  $I = 1$  channels [27]. Tornqvist could not predict whether the  $1^{++}$  state was just barely bound or not quite bound, because his results depended on an ultraviolet cutoff whose value was estimated to be the same as the corresponding ultraviolet cutoff for the two-nucleon system [27]. He also could not predict whether the state would be closer to the  $D^{*0}\bar{D}^0$  threshold or the  $D^{*+}D^-$  threshold, because his calculations were carried out in the isospin symmetry limit. With the discovery of the  $X(3872)$ , the ambiguity associated with the ultraviolet cutoff can be removed by using the observed binding energy of the  $X(3872)$  to tune the value of the ultraviolet cutoff. One can then use the meson potential model to predict the binding energies of other heavy meson molecules in both the charm sector and the bottom sector [23].

In the absence of explicit calculations of the parameters  $\gamma_0$  and  $\gamma_1$ , one can still use results of the meson potential model calculations in Ref. [27] to get some idea of the likely values of these parameters. The bound state near threshold with  $I = 0$  and  $J^{PC} = 1^{++}$  arises from the effects of coupled S-wave and D-wave channels. In the S-wave channel, the pion-exchange potential is not deep enough to give a bound state. The D-wave interaction provides just enough additional attraction to obtain a bound state very near threshold. Thus we expect  $|\gamma_0|$  to be significantly smaller than the natural scale  $m_\pi$ . The sign of  $\gamma_0$  could be either positive or negative. The meson potential model calculations in Ref. [27] indicate that there is no bound state with  $I = 1$  and  $J^{PC} = 1^{++}$ . The pion-exchange potential has the opposite

sign as in the  $I = 0$  case, so it is repulsive. We therefore expect  $\gamma_1$  to be positive and comparable to or larger than the natural scale  $m_\pi$ . In particular,  $\gamma_1$  should be much larger than  $|\gamma_0|$ . Given an estimate of  $\gamma_1$ , an estimate of  $\gamma_0$  is actually superfluous because it can be determined using Eq. (34).

The scattering amplitudes  $f_{ij}(E)$  in Eqs. (29) simplify if the parameter  $\gamma_1$  is assumed to be large compared to  $\kappa_1(0)$ . The denominator  $D(E)$  given in Eq. (30) reduces to

$$D(E) \approx -\gamma_1 [-2\gamma_0 + \kappa(E) + \kappa_1(E)]. \quad (40)$$

The scattering amplitudes reduce to

$$f_{ij}(E) \approx \frac{1}{-2\gamma_0 + \kappa_1(E) + \kappa(E)} \begin{pmatrix} 1 & -1 \\ -1 & 1 \end{pmatrix}_{ij}. \quad (41)$$

The matrix projects onto the  $I = 0$  channel. The denominator in Eq. (40) vanishes at  $E_{\text{pole}}$ . If the small difference between  $\kappa_1(E_{\text{pole}})$  and  $\kappa_1(0)$  is neglected, we get an approximate expression for  $\gamma_0$  in terms of the variable  $\gamma$  defined by Eq. (32):

$$\gamma_0 \approx \frac{\kappa_1(0) + \gamma}{2}. \quad (42)$$

In Ref. [25], the authors analyzed data from the Belle and Babar Collaborations on the energy distributions of  $J/\psi \pi^+ \pi^-$  and  $D^0 \bar{D}^0 \pi^0$  near the  $X(3872)$  resonance produced by the decay  $B^+ \rightarrow K^+ + X$ . Their model for the  $(D^* \bar{D})_+^0$  elastic scattering amplitude  $f(E)$  is a generalization of the Flatté parametrization for a near-threshold resonance [28]:

$$f_{\text{HKKN}}(E) = \frac{1}{-(2/g)[E - E_f + i\Gamma(E)/2] + \kappa_1(E) + \kappa(E)}, \quad (43)$$

where  $\kappa(E) = (-2M_{*00}E - i\varepsilon)^{1/2}$  and  $\kappa_1(E) = (-2M_{*00}(E - \nu) - i\varepsilon)^{1/2}$ . The function  $\Gamma(E)$  is determined up to normalization factors by the decays of  $X(3872)$ . The other adjustable parameters are  $g$  and  $E_f$ . In Ref. [25], the authors found that their fits had a scaling behavior that made it impossible to determine unique values of the parameters. As pointed out in Ref. [22], the scaling behavior simply indicates that their fits were insensitive to the term  $-(2/g)E$  in the denominator in Eq. (43). If this term is deleted and if  $-(2/g)E_f$  and  $\Gamma(E)/g$  are identified with the real and imaginary parts of  $2\gamma_0$ , the scattering amplitude in Eq. (43) reduces to the amplitude  $f_{00}(E)$  in Eq. (41), except that it does not take into account the effects of the  $D^*$  widths. As pointed out in Ref. [26], the  $D^{*0}$  width can be taken into account by replacing  $\kappa(E)$  by the expression in Eq. (18). Similarly, the  $D^{*+}$  width can be taken into account by replacing  $\kappa_1(E)$  by the expression in Eq. (26).

#### IV. LINE SHAPES OF $X(3872)$

If a set of particles  $C$  has total quantum numbers that are compatible with those of the  $X(3872)$  resonance and if the total energy  $E$  of these particles can be near the  $D^{*0} \bar{D}^0$  threshold, then there can be a resonant enhancement in the channel  $C$ . The line shape of  $X(3872)$  in the channel  $C$  is the differential rate for producing the particles  $C$  as a function of their total energy  $E$ . In Ref. [20], it was pointed out that the line shapes of the  $X(3872)$  can

be factored into short-distance factors that are insensitive to  $E$  and the inverse scattering length  $\gamma$  and a long-distance factor that is determined by  $E$  and  $\gamma$ . In Ref. [22], it was shown that the factorization formulas could be derived using the operator product expansion for an effective field theory that describes the  $c\bar{c}$  sector of QCD near the  $D^{*0}\bar{D}^0$  threshold. There is a factorization associated with the creation of the charm mesons if all the particles in the initial state and if the particles in the final state other than the resonating particles in  $C$  have momenta in the resonance rest frame that are of order  $m_\pi$  or larger. If  $C$  is a short-distance decay mode of  $X$ , there is also a factorization associated with the inelastic scattering of the charm mesons into the particles in  $C$ . A *short-distance* decay mode of  $X(3872)$  is one for which all the particles have momenta that are of order  $m_\pi$  or larger in the resonance rest frame. Examples of short-distance decay modes are  $J/\psi \pi^+ \pi^-$  and  $J/\psi \pi^+ \pi^- \pi^0$ . An example of a decay mode that is not short-distance is  $D^0 \bar{D}^0 \pi^0$ .

In this section, we consider the line shapes in the decays  $B \rightarrow K + C$ , where  $C$  is a channel that is enhanced by the  $X(3872)$  resonance. We first summarize the results of Ref. [26] in which only the neutral channel  $(D^* \bar{D})_+^0$  defined in Eq. (11a) was taken into account. These results should be accurate when the energy  $E$  is within a few MeV of the  $D^{*0} \bar{D}^0$  threshold. We then extend the region of validity to the entire  $D^* \bar{D}$  threshold region by taking into account the resonant coupling to the charged channel  $(D^* \bar{D})_+^1$  defined in Eq. (11b).

### A. Neutral channel only

Expressions for the line shapes of the  $X(3872)$  that take into account the  $D^{*0}$  width and inelastic scattering in the  $(D^* \bar{D})_+^0$  channel were derived in Ref. [26]. We give here a more explicit derivation of the line shapes produced by the decay  $B^+ \rightarrow K^+ + X$ . Our starting point is the optical theorem for the width of the  $B^+$ :

$$\Gamma[B^+] = -\frac{1}{M_B} \text{Im} \mathcal{A}[B^+ \rightarrow B^+], \quad (44)$$

where  $\mathcal{A}[B^+ \rightarrow B^+]$  is the one-meson-irreducible forward amplitude for  $B^+$ . This amplitude has contributions from intermediate states consisting of a  $K^+$  recoiling against sets of particles whose invariant mass  $M_{*0} + M_0 + E$  is near the  $D^{*0} \bar{D}^0$  threshold. There is resonant enhancement for small  $E$  if the particles are accessible from the  $(D^* \bar{D})_+^0$  channel. The resonant contributions to the forward amplitude can be expressed as a loop integral over the 4-momentum  $P_k$  of the  $K^+$ :

$$\mathcal{A}_{\text{res}}[B^+ \rightarrow B^+] = - \int \frac{d^4 P_K}{(2\pi)^4} \left( C_{B^+}^{K^+} f(E) C_{B^+}^{K^+} \right) \frac{i}{P_K^2 - m_K^2 + i\varepsilon}. \quad (45)$$

There is an implicit restriction of the integral to the region of small  $E$ . The expression inside the parentheses takes into account the amplitude for the creation of charm mesons in the channel  $(D^* \bar{D})_+^0$ , the resonant propagation of the pair of charm mesons, and the amplitude for their annihilation. Factorization has been used to express it as the product of a long-distance factor and two short-distance factors. The long-distance factor  $f(E)$  is the scattering amplitude for elastic scattering in the  $(D^* \bar{D})_+^0$  channel given in Eq. (14). The short-distance factors  $C_{B^+}^{K^+}$  depend on the 4-momenta  $P_B$  and  $P_K$  of the  $B^+$  and  $K^+$ , but they are insensitive to the small energy  $E$  defined by  $(P_B - P_K)^2 = (M_{*0} + M_0 + E)^2$ . The short-distance factors can therefore be simplified by setting  $E = 0$ . Using the Cutkosky

cutting rules, the resonant contribution to the imaginary part of the forward amplitude can be written

$$\text{Im}\mathcal{A}_{\text{res}}[B^+ \rightarrow B^+] = - \int \frac{d^3 P_K}{(2\pi)^3 2E_K} \left( \mathcal{C}_{B^+}^{K^+} \text{Im} f(E) (\mathcal{C}_{B^+}^{K^+})^* \right). \quad (46)$$

Again there is an implied restriction of the integral to the region of small  $E$ . The contribution to the width of  $B^+$  from its decay into  $K^+$  and the  $X(3872)$  resonance can be obtained by inserting Eq. (46) into Eq. (44). The distribution in the invariant mass  $M = M_{*0} + M_0 + E$  of the resonance can be obtained by inserting the identity

$$1 = \int d^4 P_R \delta^4(P_B - P_K - P_R) \int dM^2 \delta(M^2 - P_R^2). \quad (47)$$

Changing the order of integration and using  $E_B - E_K > 0$  and  $|E| \ll M_{*0} + M_0$ , this can be written

$$1 = \frac{M_{*0} + M_0}{\pi} \int dE \int \frac{d^3 P_R}{(2\pi)^3 2E_R} (2\pi)^4 \delta^4(P_B - P_K - P_R). \quad (48)$$

Upon inserting this into Eq. (46), we obtain a factorization formula for the inclusive energy distribution summed over all resonant channels:

$$\frac{d\Gamma}{dE}[B^+ \rightarrow K^+ + \text{resonant}] = 2 \Gamma_{B^+}^{K^+} \text{Im} f(E). \quad (49)$$

The short-distance factor is a positive real constant:

$$\Gamma_{B^+}^{K^+} = \frac{M_{*0} + M_0}{2\pi M_B} \int \frac{d^3 P_k}{(2\pi)^3 2E_R} \int \frac{d^3 P_K}{(2\pi)^3 2E_R} (2\pi)^4 \delta^4(P_B - P_k - P_R) |\mathcal{C}_{B^+}^{K^+}|^2. \quad (50)$$

A more explicit expression for the short-distance factor can be obtained by using Lorentz invariance to express the short-distance factor  $\mathcal{C}_{B^+}^{K^+}$  in the form

$$\mathcal{C}_{B^+}^{K^+} = C_{B^+}^{K^+} P_B \cdot (\epsilon_{D^*})^*, \quad (51)$$

where  $\epsilon_{D^*}$  is a polarization vector for the  $D^{*0}$  [18, 19] and  $C_{B^+}^{K^+}$  is a constant with dimensions of inverse mass. Evaluating the phase space integral and summing over the  $D^{*0}$  spins, we get

$$\Gamma_{B^+}^{K^+} = \frac{\lambda^{3/2}(M_B, m_K, M_{*0} + M_0)}{64\pi^2(M_{*0} + M_0)M_B^3} \left| C_{B^+}^{K^+} \right|^2. \quad (52)$$

The optical theorem in Eq. (15) can be used to resolve the inclusive resonant rate in Eq. (49) into two terms according to whether they have  $\text{Im}\gamma$  or  $\text{Im}\kappa(E)$  as a factor. We interpret the term proportional to  $\text{Im}\gamma$  as the contribution from all short-distance decay channels  $C$ . The imaginary part of  $\gamma$  can be expressed as a sum over those decay channels:

$$\text{Im}\gamma = \sum_C \Gamma^C(E). \quad (53)$$

We have allowed for the possibility that the dependence of some of the short-distance factors  $\Gamma^C(E)$  on the energy  $E$  may not be negligible in the  $D^{*0}\bar{D}^0$  threshold region. Thus the energy distribution in a specific short-distance channel  $C$  can be expressed as

$$\frac{d\Gamma}{dE}[B^+ \rightarrow K^+ + C] = 2 \Gamma_{B^+}^{K^+} |f(E)|^2 \Gamma^C(E). \quad (54)$$

We interpret the term in Eq. (49) proportional to  $\text{Im}\kappa(E)$  as the contribution from channels that correspond to  $D^{*0}\bar{D}^0$  or  $D^0\bar{D}^{*0}$  followed by the decay of the  $D^{*0}$  or  $\bar{D}^{*0}$ . We can resolve this term into the contributions from the channels  $D^0\bar{D}^0\pi^0$ ,  $D^+\bar{D}^0\pi^-$ ,  $D^0D^-\pi^+$ , and  $D^0\bar{D}^0\gamma$  by multiplying it by the energy-dependent branching fractions  $\text{Br}_{000}(E)$ ,  $\frac{1}{2}\text{Br}_{011}(E)$ ,  $\frac{1}{2}\text{Br}_{011}(E)$ , and  $\text{Br}_{00\gamma}(E)$ , which add up to 1. A simple expression for  $\text{Im}\kappa(E)$  can be obtained by using the identity in Eq. (19). The resulting expression for the energy distribution in the  $D^0\bar{D}^0\pi^0$  channel is

$$\frac{d\Gamma}{dE}[B^+ \rightarrow K^+ + D^0\bar{D}^0\pi^0] = 2\Gamma_{B^+}^{K^+} |f(E)|^2 \left[ M_{*00}(\sqrt{E^2 + \Gamma_{*0}(E)^2/4} + E) \right]^{1/2} \text{Br}_{000}(E), \quad (55)$$

where  $\text{Br}_{000}(E)$  is given in Eq. (10a).

The energy distributions of the  $X$  resonance in the decays  $B^0 \rightarrow K^0 + X$  are given by expressions identical to those in Eqs. (49), (54), and (55) except that the short-distance constant  $\Gamma_{B^+}^{K^+}$  is replaced by  $\Gamma_{B^0}^{K^0}$ . Thus the line shapes for  $X(3872)$  produced in  $B^+$  decays and  $B^0$  decays are predicted to be identical in the region within a few MeV of the  $D^{*0}\bar{D}^0$  threshold.

In Ref. [21], the decay rates of  $X$  into  $J/\psi$  plus  $\pi^+\pi^-$ ,  $\pi^+\pi^-\pi^0$ ,  $\pi^0\gamma$ , and  $\gamma$  were calculated under the assumption that these decays proceed through couplings of the  $X$  to  $J/\psi$  and the vector mesons  $\rho^0$  and  $\omega$ . The results of Ref. [21] were used in Ref. [26] to calculate the dependence of the factor  $\Gamma^C(E)$  in Eq. (54) on the energy  $E$  for  $C = J/\psi\pi^+\pi^-$  and  $J/\psi\pi^+\pi^-\pi^0$ . The normalization factors  $\Gamma^C(0)$  can only be determined by measurements of  $X(3872)$  decays. Simple analytic approximations to  $\Gamma^C(E)/\Gamma^C(0)$  that are accurate to within 1% in the region  $|E| < 8.5$  MeV for  $J/\psi\pi^+\pi^-$  and in the region  $|E| < 1$  MeV for  $J/\psi\pi^+\pi^-\pi^0$  are given in Ref. [26].

In Figs. 2 and 3, we illustrate the line shapes for  $X(3872)$  near the  $D^{*0}\bar{D}^0$  threshold. We take into account the  $D^{*0}$  width, but we neglect the effect on the line shapes of inelastic scattering channels for the charm mesons. We show the line shapes for three values of  $\gamma$ : +34, 0, and -34 MeV. For  $\gamma = +34$  MeV, the peak of the resonance is at  $E = -0.6$  MeV, which is the central value of the measurement in Eq. (1). In Fig. 2, we show the line shapes in a short-distance decay mode, such as  $J/\psi\pi^+\pi^-\pi^0$  or  $J/\psi\pi^+\pi^-$ . The line shape is given by Eq. (54). We have neglected the energy-dependence of the factor  $\Gamma^C(E)$ . The relative normalizations of the curves for the three values of  $\gamma$  are determined by using the same short-distance factors  $\Gamma_{B^+}^{K^+}$  and  $\Gamma^C$ . For  $\gamma = +34$  MeV, which corresponds to a bound state, the line shape is dominated by the Breit-Wigner resonance near  $E = -0.6$  MeV. For  $\gamma = -34$  MeV, which corresponds to a virtual state, the line shape has a cusp near  $E = 0$  MeV. In Fig. 3, we show the line shapes in the  $D^0\bar{D}^0\pi^0$  channel. The line shape is given by Eq. (55). The relative normalizations of the curves for the three values of  $\gamma$  are determined by using the same short-distance factor  $\Gamma_{B^+}^{K^+}$ . For  $\gamma = +34$  MeV, which corresponds to a bound state, the dominant features of the line shape are a Breit-Wigner resonance near  $E = -0.6$  MeV and a threshold enhancement for  $E > 0$ . For  $\gamma = -34$  MeV, which corresponds to a virtual state, the line shape has only the threshold enhancement.

## B. Coupled neutral and charged channels

We proceed to generalize the factorization formulas in Section IV A to the two-channel case. We begin by generalizing the forward amplitude in Eq. (45). We have to take into



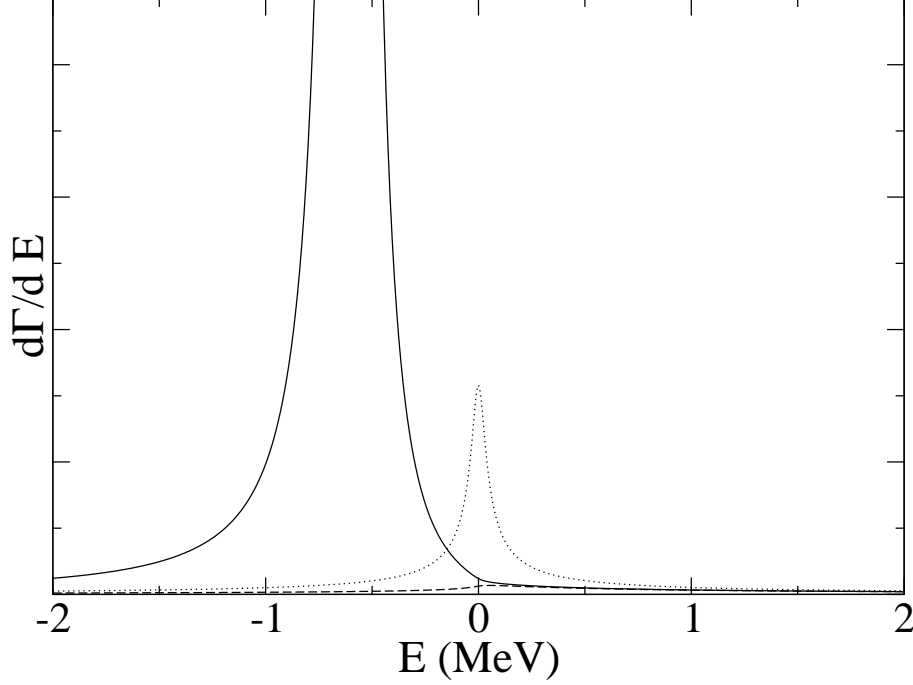


FIG. 2: The line shapes near the  $D^{*0}\bar{D}^0$  threshold for  $X(3872)$  decaying into a short-distance channel, such as  $J/\psi \pi^+\pi^-$  or  $J/\psi \pi^+\pi^-\pi^0$ . The line shapes are shown for three values of  $\gamma$ : +34 MeV (solid line), 0 (dotted line), and -34 MeV (dashed line).

account the possibility of resonant scattering between any pair of the charged and neutral channels. The amplitude can be written

$$\mathcal{A}_{\text{res}}[B^+ \rightarrow B^+] = - \int \frac{d^4 P_K}{(2\pi)^4} \sum_{i=0}^1 \sum_{j=0}^1 \left( \mathcal{C}_{B^+}^{K^+,i} f_{ij}(E) \mathcal{C}_{B^+}^{K^+,j} \right) \frac{i}{P_K^2 - m_K^2 + i\varepsilon}. \quad (56)$$

Following the same path as in Section IV A, we ultimately arrive at a factorization formula for the inclusive energy distribution summed over all resonant channels:

$$\frac{d\Gamma}{dE}[B^+ \rightarrow K^+ + \text{resonant}] = 2 \sum_{i=0}^1 \sum_{j=0}^1 \Gamma_{B^+}^{K^+,ij} \text{Im} f_{ij}(E). \quad (57)$$

The short-distance factors are

$$\Gamma_{B^+}^{K^+,ij} = \frac{M_{*0} + M_0}{2\pi M_B} \int \frac{d^3 P_R}{(2\pi)^3 2E_R} \int \frac{d^3 P_K}{(2\pi)^3 2E_K} (2\pi)^4 \delta^4(P_B - P_K - P_R) \mathcal{C}_{B^+}^{K^+,i} (\mathcal{C}_{B^+}^{K^+,j})^*. \quad (58)$$

The short-distance factors  $\Gamma_{B^+}^{K^+,00}$  and  $\Gamma_{B^+}^{K^+,11}$  are positive real constants, while  $\Gamma_{B^+}^{K^+,01} = (\Gamma_{B^+}^{K^+,10})^*$  is a complex constant. Thus there are four independent real constants associated with the  $B^+ \rightarrow K^+$  transitions. These constants satisfy the Schwarz inequality

$$\left| \Gamma_{B^+}^{K^+,01} \right|^2 \leq \Gamma_{B^+}^{K^+,00} \Gamma_{B^+}^{K^+,11}. \quad (59)$$

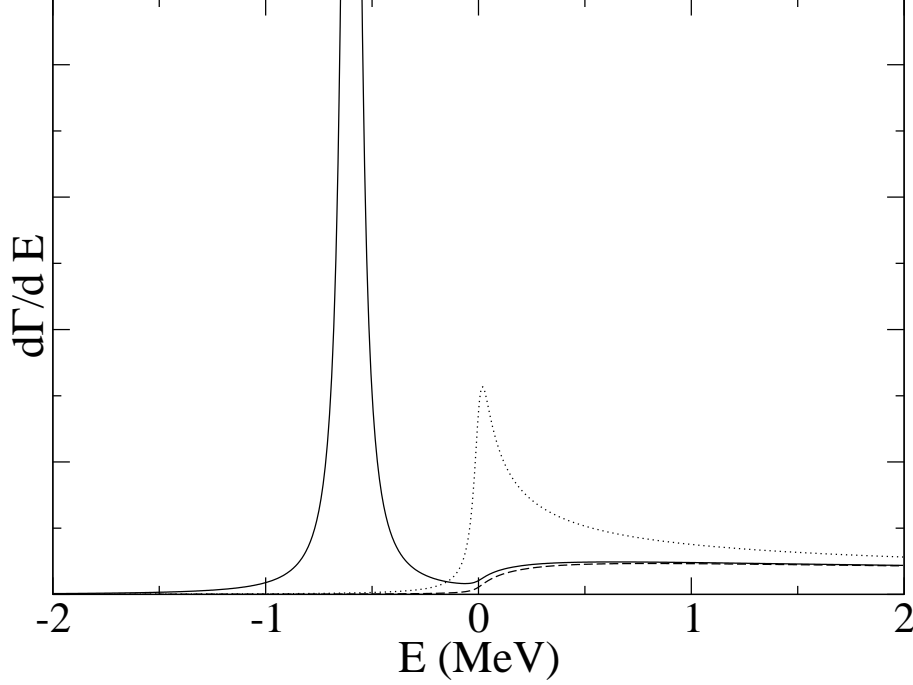


FIG. 3: The line shapes near the  $D^{*0}\bar{D}^0$  threshold for  $X(3872)$  in the  $D^0\bar{D}^0\pi^0$  channel. The line shapes are shown for three values of  $\gamma$ : +34 MeV (solid line), 0 (dotted line), and -34 MeV (dashed line).

The optical theorem in Eq. (31) can be used to resolve the inclusive resonant rate in Eq. (57) into four terms according to whether they have  $\text{Im}\gamma_0$ ,  $\text{Im}\gamma_1$ ,  $\text{Im}\kappa(E)$ , or  $\text{Im}\kappa_1(E)$  as a factor. We interpret the terms proportional to  $\text{Im}\gamma_0$  and  $\text{Im}\gamma_1$  as the contributions from short-distance decay channels  $C$ . The imaginary parts of  $\gamma_0$  and  $\gamma_1$  can be expressed as sums over those decay channels:

$$\text{Im}\gamma_0 = \sum_C \Gamma_0^C(E), \quad (60a)$$

$$\text{Im}\gamma_1 = \sum_C \Gamma_1^C(E). \quad (60b)$$

The factorization formula for the energy distribution in a specific short-distance decay channel  $C$  is

$$\begin{aligned} \frac{d\Gamma}{dE}[B^+ \rightarrow K^+ + C] = & \left( \sum_{i=0}^1 \sum_{j=0}^1 \Gamma_{B^+}^{K^+,ij} [f_{i0}(E) - f_{i1}(E)][f_{j0}^*(E) - f_{j1}^*(E)] \right) \Gamma_0^C(E) \\ & + \left( \sum_{i=0}^1 \sum_{j=0}^1 \Gamma_{B^+}^{K^+,ij} [f_{i0}(E) + f_{i1}(E)][f_{j0}^*(E) + f_{j1}^*(E)] \right) \Gamma_1^C(E). \end{aligned} \quad (61)$$

The terms in Eq. (57) proportional to  $\text{Im}\kappa(E)$  and  $\text{Im}\kappa_1(E)$  also have simple interpretations. We interpret the term proportional to  $\text{Im}\kappa(E)$  as the contribution from channels that correspond to  $D^{*0}\bar{D}^0$  or  $D^0\bar{D}^{*0}$  followed by the decay of the  $D^{*0}$  or  $\bar{D}^{*0}$ . We can resolve this term into the contributions from the individual channels  $D^0\bar{D}^0\pi^0$ ,  $D^+\bar{D}^0\pi^-$ ,  $D^0D^-\pi^+$ , and

$D^0 \bar{D}^0 \gamma$  by multiplying it by the energy-dependent branching fractions  $\text{Br}_{000}(E)$ ,  $\frac{1}{2}\text{Br}_{011}(E)$ , and  $\frac{1}{2}\text{Br}_{011}(E)$ , and  $\text{Br}_{00\gamma}(E)$ , which add up to 1. For example, the line shape of  $X$  in the  $D^0 \bar{D}^0 \pi^0$  decay mode is

$$\begin{aligned} \frac{d\Gamma}{dE}[B^+ \rightarrow K^+ + D^0 \bar{D}^0 \pi^0] &= 2 \left( \sum_{i=0}^1 \sum_{j=0}^1 \Gamma_{B^+}^{K^+,ij} f_{i0}(E) f_{j0}^*(E) \right) \\ &\times \left[ M_{*00} (\sqrt{E^2 + (\Gamma_{*0}(E)/2)^2} + E) \right]^{1/2} \text{Br}_{000}(E), \quad (62) \end{aligned}$$

where  $\text{Br}_{000}(E)$  is given in Eq. (10a). We interpret the term in Eq. (57) proportional to  $\text{Im}\kappa_1(E)$  as the contribution from channels that correspond to  $D^{*+}D^-$  or  $D^+D^{*-}$  followed by the decay of the  $D^{*+}$  or  $D^{*-}$ . We can resolve this term into the contributions from the individual channels  $D^+D^-\pi^0$ ,  $D^0D^-\pi^+$ ,  $D^+\bar{D}^0\pi^-$ , and  $D^+D^-\gamma$  by multiplying it by energy-dependent branching fractions. For example, the line shape of  $X$  in the  $D^+D^-\pi^0$  decay mode is

$$\begin{aligned} \frac{d\Gamma}{dE}[B^+ \rightarrow K^+ + D^+D^-\pi^0] &= 2 \left( \sum_{i=0}^1 \sum_{j=0}^1 \Gamma_{B^+}^{K^+,ij} f_{i1}(E) f_{j1}^*(E) \right) \\ &\times \left[ M_{*11} (\sqrt{(E-\nu)^2 + (\Gamma_{*1}(E-\nu)/2)^2} + E - \nu) \right]^{1/2} \text{Br}_{110}(E), \quad (63) \end{aligned}$$

where  $\text{Br}_{110}(E)$  is given in Eq. (10b). The expressions for the line shapes in the decay channels  $D^0D^-\pi^+$  and  $D^-D^0\pi^+$  are more complicated because they receive contributions from channels that correspond to  $D^{*0}\bar{D}^0$  or  $D^0\bar{D}^{*0}$  as well as channels that correspond to  $D^{*+}D^-$  or  $D^+D^{*-}$ .

If the energy  $E$  is very close to the  $D^{*0}\bar{D}^0$  threshold, the two-channel factorization formulas in Eqs. (57), (61), and (62) should reduce to the single-channel factorization formulas in Eqs. (49), (54), and (55). For the factorization formula for  $B^+ \rightarrow K^+ + D^0 \bar{D}^0 \pi^0$  in Eq. (62), this can be verified by inserting the expressions in Eq. (38) for the scattering amplitudes  $f_{ij}(E)$  at small  $E$ . The factorization formula reduces to Eq. (55) with the short-distance factor  $\Gamma_{B^+}^{K^+}$  given by

$$\Gamma_{B^+}^{K^+} \approx \sum_{i=0}^1 \sum_{j=0}^1 \Gamma_{B^+}^{K^+,ij} c_i c_j^*. \quad (64)$$

Similarly, the factorization formula for  $B^+ \rightarrow K^+ + C$  in Eq. (61) reduces to Eq. (54) with  $\Gamma_{B^+}^{K^+}$  given by Eq. (64) and  $\Gamma^C(E)$  given by

$$\Gamma^C(E) \approx \frac{|1 - c_1|^2}{2} \Gamma_0^C(E) + \frac{|1 + c_1|^2}{2} \Gamma_1^C(E). \quad (65)$$

To see that the two-channel factorization formula in Eq. (57) for the inclusive resonant rate reduces to Eq. (49), we express the imaginary part of  $f_{ij}(E)$  in a form that is compatible with the Cutkosky cutting rules:

$$\text{Im}f_{ij}(E) = c_i f(E) (\text{Im}c_j) + c_i (\text{Im}f(E)) c_j^* + (\text{Im}c_i) f^*(E) c_j^*. \quad (66)$$

Since  $c_0 = 1$ , it has no imaginary part. The expression for  $c_1$  in Eq. (39b) is a function of  $\gamma_1$  and  $\kappa_1(0)$  only. The imaginary part of  $\kappa_1(0)$  is suppressed relative to its real part by a

factor of  $\Gamma[D^{*+}]/\nu$ . We expect  $\gamma_1$  to have a real part that is comparable to or larger than  $m_\pi$ , so the imaginary part of  $\gamma_1$  should also be small relative to its real part. Thus the only term on the right side of Eq. (66) that is not suppressed is the one with the factor  $\text{Im}f(E)$ . Inserting that term into the factorization formula in Eq. (57), we find that it reduces to Eq. (49) with  $\Gamma_{B^+}^{K^+}$  given by Eq. (64).

The factorization formulas for the energy distributions simplify if the parameter  $\gamma_1$  is assumed to be large compared to  $\kappa_1(0)$ . The scattering amplitudes  $f_{ij}(E)$  in Eq. (29) reduce to the expressions in Eq. (41). The two-channel factorization formula in Eqs. (57), (61), and (62) all reduce to the single-channel factorization formulas in Eqs. (49), (54), and Eq. (55) with the scattering amplitude  $f(E)$  replaced by the expression for  $f_{00}(E)$  given in Eq. (41). By using Eq. (42) to eliminate  $\gamma_0$  in favor of  $\gamma$ , the scattering amplitude reduces to

$$f(E) \approx \frac{1}{-\gamma + \kappa(E) + \kappa_1(E) - \kappa_1(0)}. \quad (67)$$

The short-distance factor for  $B^+ \rightarrow K^+$  transitions reduces to

$$\Gamma_{B^+}^{K^+} \approx \sum_{i=0}^1 \sum_{J=0}^1 (-1)^{i+J} \Gamma_{B^+}^{K^+,ij}. \quad (68)$$

The sums project the  $(D^*\bar{D})_+$  channels onto isospin 0. The short-distance factor for the short-distance decay channel reduces to

$$\Gamma^C(E) \approx 2\Gamma_0^C(E). \quad (69)$$

The coefficient of  $\Gamma_1^C(E)$  goes to zero in this limit. Thus the decay of  $X$  into final states  $C$  with total isospin quantum number  $I = 1$ , such as  $J/\psi \pi^+ \pi^-$ , are suppressed in the large- $\gamma_1$  limit.

### C. Constraints from isospin symmetry

We have not yet fully exploited the approximate isospin symmetry of QCD. Since the short-distance factors only involve momenta of order  $m_\pi$  and larger, isospin-violating effects can be neglected in these factors. Thus isospin symmetry can be used to constrain the short-distance factors. At the quark level, the transitions  $B \rightarrow K + D^*\bar{D}$  and  $B \rightarrow K + D\bar{D}^*$  proceed through two operators in the effective weak Hamiltonian: the charged current operator  $\bar{b}\gamma^\mu(1-\gamma_5)c \bar{c}\gamma_\mu(1-\gamma_5)s$  and the neutral current operator  $\bar{b}\gamma^\mu(1-\gamma_5)s \bar{c}\gamma_\mu(1-\gamma_5)c$ . These operators are both isospin singlets. Thus isospin symmetry is respected by these transitions. It can therefore be used to relate the short-distance coefficients  $\mathcal{C}_{B^+}^{K^+,i}$  for the  $B^+ \rightarrow K^+$  transition to the short-distance coefficients  $\mathcal{C}_{B^0}^{K^0,i}$  for the  $B^0 \rightarrow K^0$  transition. Since  $B^+$  and  $B^0$  form an isospin doublet and  $K^+$  and  $K^0$  form an isospin doublet, the coefficients  $\mathcal{C}_{B^0}^{K^0,i}$  and  $\mathcal{C}_{B^+}^{K^+,i}$  are related by Clebsch-Gordan coefficients:

$$\mathcal{C}_{B^0}^{K^0,0} = -\mathcal{C}_{B^+}^{K^+,1}, \quad (70a)$$

$$\mathcal{C}_{B^0}^{K^0,1} = -\mathcal{C}_{B^+}^{K^+,0}. \quad (70b)$$

This implies that the short-distance constants  $\Gamma_{B^0}^{K^0,ij}$  in the factorization formulas for  $B^0 \rightarrow K^0$  transitions are related to the corresponding constants  $\Gamma_{B^+}^{K^+,ij}$  in the factorization formulas for  $B^+ \rightarrow K^+$  transitions by

$$\Gamma_{B^0}^{K^0,00} = \Gamma_{B^+}^{K^+,11}, \quad (71a)$$

$$\Gamma_{B^0}^{K^0,01} = (\Gamma_{B^+}^{K^+,01})^*, \quad (71b)$$

$$\Gamma_{B^0}^{K^0,11} = \Gamma_{B^+}^{K^+,00}. \quad (71c)$$

Thus the short-distance constants associated with the  $B^+ \rightarrow K^+$  and  $B^0 \rightarrow K^0$  transitions are determined by four independent real constants.

Isospin symmetry also constrains the short-distance factors  $\Gamma_I^C(E)$  associated with decays of  $X$  into short-distance decay modes. It implies that for a decay channel  $C$  with definite isospin quantum number  $I = 0$  or  $I = 1$ , only the term with the factor  $\Gamma_I(E)$  contributes. An example of a decay channel with isospin quantum number  $I = 0$  is  $J/\psi \pi^+ \pi^- \pi^0$ , assuming that the  $\pi^+ \pi^- \pi^0$  comes from the decay of a virtual  $\omega$ . An example of a decay channel with isospin quantum number  $I = 1$  is  $J/\psi \pi^+ \pi^-$ , assuming that the  $\pi^+ \pi^-$  comes from the decay of a virtual  $\rho^0$ . We will give the factorization formulas for short-distance decay channels with definite isospin quantum number  $I = 0$  and  $I = 1$  for both  $B^+ \rightarrow K^+$  transitions and  $B^0 \rightarrow K^0$  transitions. For a short-distance decay channel  $C$  with definite isospin quantum number  $I = 0$ , such as  $J/\psi \pi^+ \pi^- \pi^0$ , the energy distribution in Eq. (61) reduces to

$$\begin{aligned} \frac{d\Gamma}{dE}[B^+ \rightarrow K^+ + C] = & 4 \left( \Gamma_{B^+}^{K^+,00} |\gamma_1 - \kappa_1(E)|^2 - 2\text{Re}[\Gamma_{B^+}^{K^+,01}(\gamma_1 - \kappa_1(E))(\gamma_1 - \kappa(E))^*] \right. \\ & \left. + \Gamma_{B^+}^{K^+,11} |\gamma_1 - \kappa(E)|^2 \right) \frac{\Gamma_0^C(E)}{|D(E)|^2}, \end{aligned} \quad (72a)$$

$$\begin{aligned} \frac{d\Gamma}{dE}[B^0 \rightarrow K^0 + C] = & 4 \left( \Gamma_{B^+}^{K^+,00} |\gamma_1 - \kappa(E)|^2 - 2\text{Re}[\Gamma_{B^+}^{K^+,01}(\gamma_1 - \kappa(E))(\gamma_1 - \kappa_1(E))^*] \right. \\ & \left. + \Gamma_{B^+}^{K^+,11} |\gamma_1 - \kappa_1(E)|^2 \right) \frac{\Gamma_0^C(E)}{|D(E)|^2}. \end{aligned} \quad (72b)$$

For a short-distance decay channel  $C$  with definite isospin quantum number  $I = 1$ , such as  $J/\psi \pi^+ \pi^-$ , the energy distribution in Eq. (61) reduces to

$$\begin{aligned} \frac{d\Gamma}{dE}[B^+ \rightarrow K^+ + C] = & 4 \left( \Gamma_{B^+}^{K^+,00} |\gamma_0 - \kappa_1(E)|^2 + 2\text{Re}[\Gamma_{B^+}^{K^+,01}(\gamma_0 - \kappa_1(E))(\gamma_0 - \kappa(E))^*] \right. \\ & \left. + \Gamma_{B^+}^{K^+,11} |\gamma_0 - \kappa(E)|^2 \right) \frac{\Gamma_1^C(E)}{|D(E)|^2}, \end{aligned} \quad (73a)$$

$$\begin{aligned} \frac{d\Gamma}{dE}[B^0 \rightarrow K^0 + C] = & 4 \left( \Gamma_{B^+}^{K^+,00} |\gamma_0 - \kappa(E)|^2 + 2\text{Re}[\Gamma_{B^+}^{K^+,01}(\gamma_0 - \kappa(E))(\gamma_0 - \kappa_1(E))^*] \right. \\ & \left. + \Gamma_{B^+}^{K^+,11} |\gamma_0 - \kappa_1(E)|^2 \right) \frac{\Gamma_1^C(E)}{|D(E)|^2}. \end{aligned} \quad (73b)$$

In Eqs. (72b) and (73b), we have used the isospin symmetry relations in Eqs. (71) to express the short-distance coefficients  $\Gamma_{B^0}^{K^0,ij}$  in terms of  $\Gamma_{B^+}^{K^+,ij}$ .

The effects of the charged charm meson channel  $(D^* \bar{D})_+^1$  on the line shapes of  $X(3872)$  in the decays  $B \rightarrow K + J/\psi \pi^+ \pi^-$  and  $B \rightarrow K + J/\psi \pi^+ \pi^- \pi^0$  have been discussed recently

by Voloshin [29]. Voloshin made conceptual errors by ignoring resonant scattering between the  $(D^*\bar{D})_+^0$  and  $(D^*\bar{D})_+^1$  channels and ignoring the constraints of isospin symmetry on the transitions  $B \rightarrow K$ . In Voloshin's paper, our parameters  $\gamma_0$  and  $\gamma_1$  are denoted by  $\kappa_0$  and  $\kappa_1$  and the analogs of our functions  $\kappa(E)$  and  $\kappa_1(E)$  are denoted by  $-ik_n$  and  $\kappa_c$ . Voloshin took into account the constraints of isospin symmetry associated with the  $J/\psi \pi^+\pi^-$  and  $J/\psi \pi^+\pi^-\pi^0$  in the final state. His results for the energy distributions can be expressed in the form

$$\frac{d\Gamma}{dE}[B \rightarrow K + J/\psi \pi^+\pi^-\pi^0] = \left| \frac{\gamma_1 - \kappa_1(E)}{D(E)} \right|^2 \Phi^{J/\psi \omega}, \quad (74a)$$

$$\frac{d\Gamma}{dE}[B \rightarrow K + J/\psi \pi^+\pi^-] = \left| \frac{\gamma_0 - \kappa_1(E)}{D(E)} \right|^2 \Phi^{J/\psi \rho}, \quad (74b)$$

where  $\kappa(E) = (-2M_{*00}E - i\varepsilon)^{1/2}$  and  $\kappa_1(E) = (-2M_{*11}(E - \nu) - i\varepsilon)^{1/2}$ . The normalizing factors  $\Phi^{J/\psi \rho}$  and  $\Phi^{J/\psi \omega}$  can presumably be different for  $B^+$  decays and  $B^-$  decays, although this was not stated explicitly in Ref. [29]. The line shapes however were predicted to be the same for  $B^+$  decays and  $B^-$  decays. Voloshin's results in Eqs. (74) correspond to specific choices for the short-distance factors  $\Gamma_{B^+}^{K^+,ij}$  in our general factorization formulas in Eqs. (72) and (73). In the case of  $B^+$  decays, his results in Eqs. (74) are consistent with our factorization formulas in Eqs. (72a) and (73a) if  $\Gamma_{B^+}^{K^+,00}$  is the only nonzero short-distance factor for the  $B \rightarrow K$  transition. In the case of  $B^0$  decays, his results in Eqs. (74) are consistent with our factorization formulas in Eqs. (72b) and (73b) if  $\Gamma_{B^+}^{K^+,11} = \Gamma_{B^0}^{K^0,00}$  is the only such nonzero factor. However these conditions for  $B^+$  decays and  $B^0$  decays are inconsistent. Thus Voloshin's results are incompatible with the constraints of isospin symmetry associated with the  $B \rightarrow K$  transitions. The primary conceptual error in Ref. [29] was the assumption that there is a resonance in the amplitude only if the  $B \rightarrow K$  transition creates the charm mesons in the neutral channel  $(D^*\bar{D})_+^0$ . However there is also a resonant contribution coming from the  $B \rightarrow K$  transition creating charm mesons in the charged channel  $(D^*\bar{D})_+^1$  followed by the resonant scattering of the charm mesons into the neutral channel. A second conceptual error in Ref. [29] was the failure to take into account the constraints of isospin symmetry on the amplitudes for the  $B \rightarrow K$  transition.

#### D. Current-current factorization and heavy-quark symmetry

In Ref. [19], it was pointed out that the combination of a standard current-current factorization approximation and heavy-quark symmetry could be used to simplify the factorization formulas associated with the  $X$  resonance in  $B \rightarrow K$  transitions. In the standard current-current factorization approximation, the matrix elements of the relevant terms in the effective weak Hamiltonian are expressed as products of matrix elements of currents:

$$\langle KD^*\bar{D}|\bar{b}\gamma^\mu(1-\gamma_5)c\bar{c}\gamma_\mu(1-\gamma_5)s|B\rangle \approx \langle \bar{D}|\bar{b}\gamma^\mu(1-\gamma_5)c|B\rangle \langle KD^*|\bar{c}\gamma_\mu(1-\gamma_5)s|0\rangle, \quad (75a)$$

$$\langle KD^*\bar{D}|\bar{b}\gamma^\mu(1-\gamma_5)s\bar{c}\gamma_\mu(1-\gamma_5)c|B\rangle \approx \langle K|\bar{b}\gamma^\mu(1-\gamma_5)s|B\rangle \langle D^*\bar{D}|\bar{c}\gamma_\mu(1-\gamma_5)c|0\rangle. \quad (75b)$$

The  $D^*$  and  $\bar{D}$  in the final state can equally well be replaced by  $D$  and  $\bar{D}^*$ . The matrix element of the charged current  $\bar{b}\gamma^\mu(1-\gamma_5)c$  in Eq. (75a) is nonzero only if the  $\bar{D}$  contains the

same light quark as the  $B$ . In the case of a  $B^+$ , the  $\bar{D}$  or  $\bar{D}^*$  must be  $\bar{D}^0$  or  $\bar{D}^{*0}$ . In the case of a  $B^0$ , the  $\bar{D}$  or  $\bar{D}^*$  must be  $D^-$  or  $D^{*-}$ . As pointed out in Ref. [19], heavy-quark symmetry implies that the matrix element of the neutral current  $\bar{c}\gamma_\mu(1-\gamma_5)c$  in Eq. (75b) vanishes at the  $D^*\bar{D}$  threshold. Thus this matrix element is suppressed in the  $D^*\bar{D}$  threshold region. Putting these two observations together, we conclude that the current-current factorization approximation together with heavy quark symmetry puts strong constraints on the matrix elements of the effective weak Hamiltonian. It implies that in  $B^+ \rightarrow K^+$  transitions, the formation of the  $X(3872)$  resonance is dominated by the creation of charm mesons at short distances in the neutral channel  $(D^*\bar{D})_+^0$ . Similarly, in  $B^0 \rightarrow K^0$  transitions, the formation of the  $X(3872)$  resonance is dominated by the creation of charm mesons at short distances in the charged channel  $(D^*\bar{D})_+^1$ . These statements imply that the short-distance coefficients  $\mathcal{C}_{B^+}^{K^+,1} = -\mathcal{C}_{B^0}^{K^0,0}$  are suppressed relative to  $\mathcal{C}_{B^+}^{K^+,0} = -\mathcal{C}_{B^0}^{K^0,1}$ . This suppression leads to a hierarchy in the short-distance factors associated with  $B \rightarrow K$  transitions in the factorization formulas:

$$\Gamma_{B^+}^{K^+,11} \ll |\Gamma_{B^+}^{K^+,01}| \ll \Gamma_{B^+}^{K^+,00}. \quad (76)$$

If we assume that  $\Gamma_{B^+}^{K^+,11}$  and  $|\Gamma_{B^+}^{K^+,01}|$  are negligible compared to  $\Gamma_{B^+}^{K^+,00}$ , the expressions for the line shapes of  $X(3872)$  become rather simple. For a short-distance decay channel  $C$  with definite isospin quantum number  $I = 0$ , such as  $J/\psi \pi^+ \pi^- \pi^0$ , the energy distributions in Eqs. (72) reduce to

$$\frac{d\Gamma}{dE}[B^+ \rightarrow K^+ + C] \approx 4 \Gamma_{B^+}^{K^+,00} \left| \frac{\gamma_1 - \kappa_1(E)}{D(E)} \right|^2 \Gamma_0^C(E), \quad (77a)$$

$$\frac{d\Gamma}{dE}[B^0 \rightarrow K^0 + C] \approx 4 \Gamma_{B^+}^{K^+,00} \left| \frac{\gamma_1 - \kappa(E)}{D(E)} \right|^2 \Gamma_0^C(E). \quad (77b)$$

For a short-distance decay channel  $C$  with definite isospin quantum number  $I = 1$ , such as  $J/\psi \pi^+ \pi^-$ , the energy distributions in Eqs. (73) reduce to

$$\frac{d\Gamma}{dE}[B^+ \rightarrow K^+ + C] \approx 4 \Gamma_{B^+}^{K^+,00} \left| \frac{\gamma_0 - \kappa_1(E)}{D(E)} \right|^2 \Gamma_1^C(E), \quad (78a)$$

$$\frac{d\Gamma}{dE}[B^0 \rightarrow K^0 + C] \approx 4 \Gamma_{B^+}^{K^+,00} \left| \frac{\gamma_0 - \kappa(E)}{D(E)} \right|^2 \Gamma_1^C(E). \quad (78b)$$

For the  $D^0 \bar{D}^0 \pi^0$  channel, the energy distribution in Eqs. (62) from the  $B^+ \rightarrow K^+$  transition and its analog from the  $B^0 \rightarrow K^0$  transition reduce to

$$\begin{aligned} \frac{d\Gamma}{dE}[B^+ \rightarrow K^+ + D^0 \bar{D}^0 \pi^0] &\approx 2 \Gamma_{B^+}^{K^+,00} \left| \frac{\gamma_1 + \gamma_0 - 2\kappa_1(E)}{D(E)} \right|^2 \\ &\times \left[ M_{*00}(\sqrt{E^2 + \Gamma_{*0}(E)^2/4} + E) \right]^{1/2} \text{Br}_{000}(E), \end{aligned} \quad (79a)$$

$$\begin{aligned} \frac{d\Gamma}{dE}[B^0 \rightarrow K^0 + D^0 \bar{D}^0 \pi^0] &\approx 2 \Gamma_{B^+}^{K^+,00} \left| \frac{\gamma_1 - \gamma_0}{D(E)} \right|^2 \\ &\times \left[ M_{*00}(\sqrt{E^2 + \Gamma_{*0}(E)^2/4} + E) \right]^{1/2} \text{Br}_{000}(E). \end{aligned} \quad (79b)$$

Note that the line shapes in Eqs. (77), (78), and (79) are determined by the parameters  $\gamma_0$  and  $\gamma_1$  or, equivalently,  $\gamma$  and  $\gamma_1$ . The relative normalizations of the rates from the  $B^0 \rightarrow K^0$  transition and from the  $B^+ \rightarrow K^+$  transition are also determined by  $\gamma$  and  $\gamma_1$ .

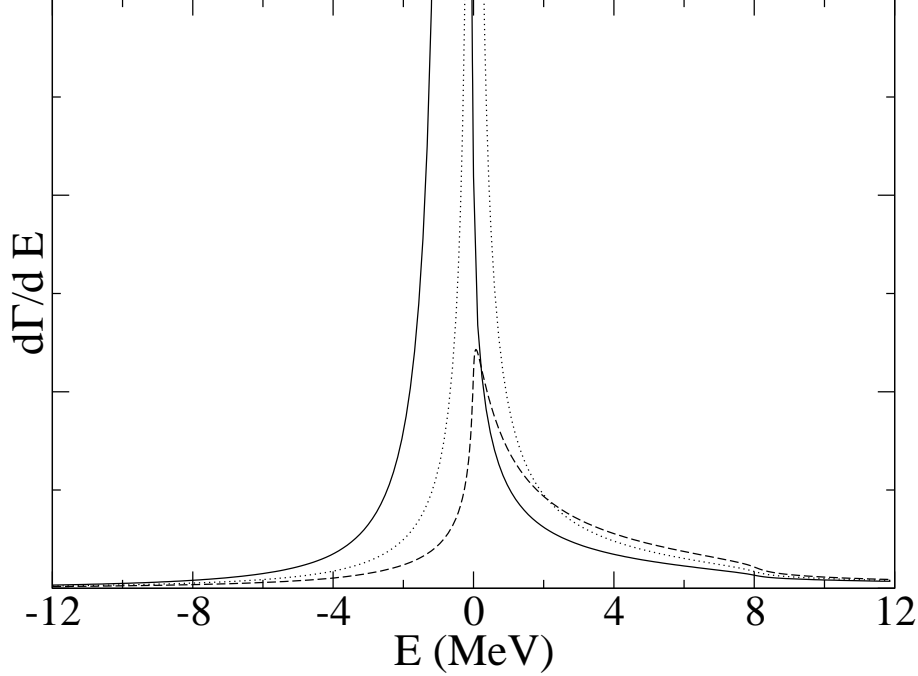


FIG. 4: The line shapes in the  $D^*\bar{D}$  threshold region for  $X(3872)$  produced by a  $B^+ \rightarrow K^+$  or  $B^0 \rightarrow K^0$  transition and decaying into  $J/\psi \pi^+ \pi^- \pi^0$ . The line shapes are shown for  $\gamma_1 = \pm\infty$  and three values of  $\gamma$ : +34 MeV (solid line), 0 (dotted line), and -34 MeV (dashed line).

In Figs. 4, 5, and 6, we illustrate the line shapes in the  $D^*\bar{D}$  threshold region for  $X(3872)$  produced by  $B \rightarrow K$  transitions. We take into account the  $D^{*0}$  width, but we neglect the effect on the line shapes of inelastic scattering channels for the charm mesons. For simplicity, we show only the line shapes for the limiting case  $\gamma_1 \rightarrow \pm\infty$ . Thus the denominators  $D(E)$  can be approximated by Eq. (40) and numerator factors such as  $\gamma_1 - \kappa_1(E)$  or  $\gamma_1 - \kappa(E)$  can be approximated by  $\gamma_1$ . The parameters  $\gamma$  and  $\gamma_0$  are related by the pole equation  $2\gamma_0 - \gamma - \kappa_1(E_{\text{pole}}) = 0$ , where  $E_{\text{pole}}$  is given in Eq. (20). If we take  $\gamma_0$  to be real, then  $\gamma$  has an unphysical negative imaginary part. We therefore take  $\gamma$  to be real and use the pole equation to determine the complex parameter  $\gamma_0$ :

$$\gamma_0 = \frac{1}{2} \left( \sqrt{2M_{*11}\nu + (M_{*11}/M_{*00})\gamma^2 + iM_{*11}(\Gamma[D^{*0}] - \Gamma_{*1}(-\nu))} + \gamma \right). \quad (80)$$

We show the line shapes for three real values of  $\gamma$ : +34, 0, and -34 MeV. The corresponding values of  $\gamma_0$  have real parts 82 MeV, 63 MeV, and 48 MeV, respectively. Their imaginary parts are all approximately 0.00012 MeV, which is completely negligible. For  $\gamma = +34$  MeV, the peak of the resonance is at  $E = -0.6$  MeV, which is the central value of the measurement in Eq. (1).

In Fig. 4, we show the line shapes in the short-distance decay mode  $J/\psi \pi^+ \pi^- \pi^0$ . The line shapes, which are the same for  $X$  produced by a  $B^+ \rightarrow K^+$  or  $B^0 \rightarrow K^0$  transition, are given in Eqs. (77). The relative normalizations of the curves for the three values of  $\gamma$  are determined by using the same short-distance factors  $\Gamma_{B^+}^{K^+,00}$  and  $\Gamma^{J/\psi \pi^+ \pi^- \pi^0}$ . In Fig. 5, we show the line shapes in the short-distance decay mode  $J/\psi \pi^+ \pi^-$ . The line shapes are given in Eqs. (78). The upper and lower panels show the line shapes produced by  $B^+ \rightarrow K^+$  and  $B^0 \rightarrow K^0$  transitions, respectively. The line shapes from the  $B^+ \rightarrow K^+$  transition have



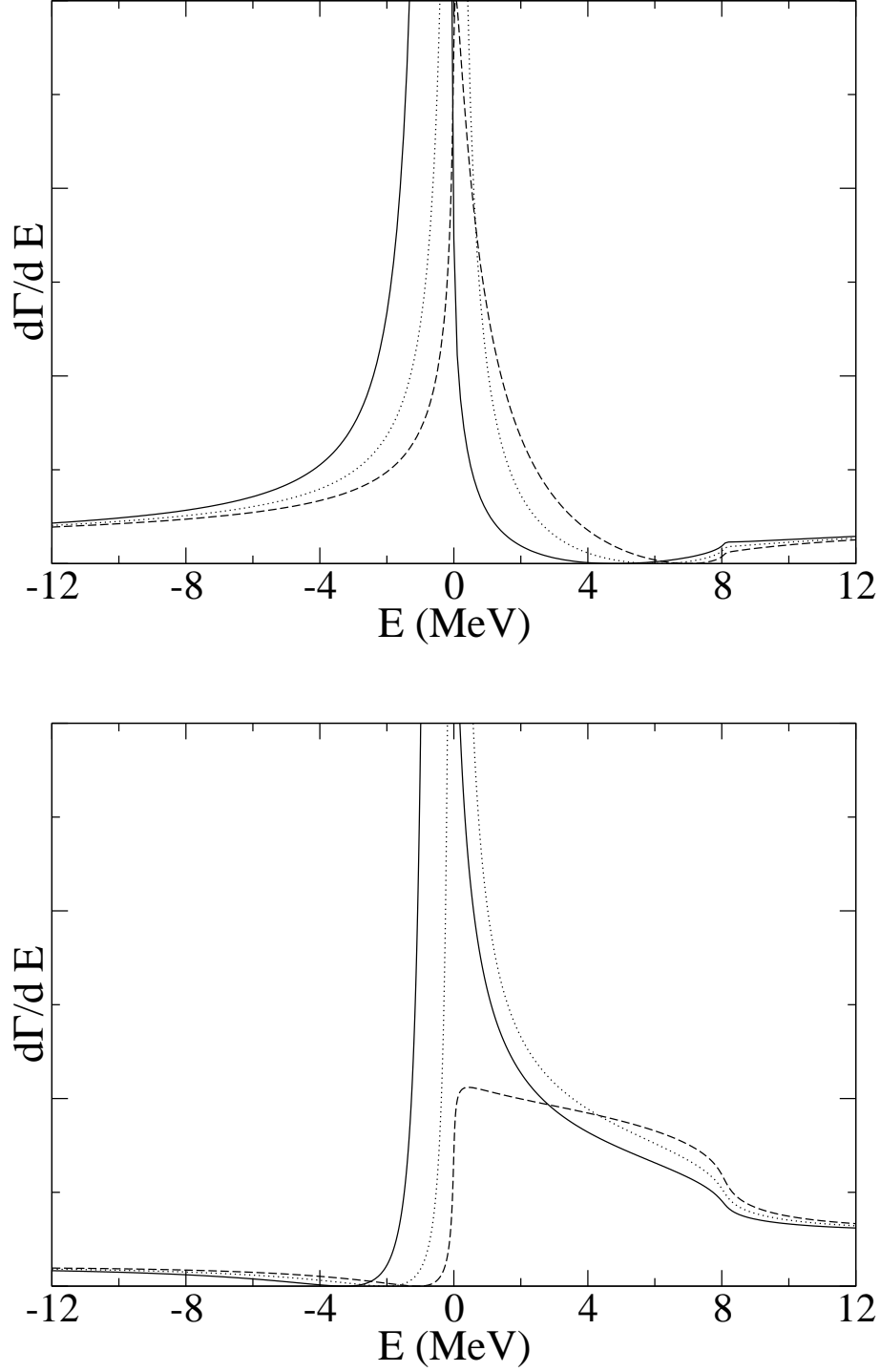


FIG. 5: The line shapes in the  $D^*\bar{D}$  threshold region for  $X(3872)$  produced by a  $B \rightarrow K$  transition and decaying into  $J/\psi \pi^+ \pi^-$ . The line shapes are different for  $X$  produced by a  $B^+ \rightarrow K^+$  transition (upper panel) and a  $B^0 \rightarrow K^0$  transition (lower panel). The line shapes are shown for  $\gamma_1 = \pm\infty$  and three values of  $\gamma$ :  $+34$  MeV (solid lines),  $0$  (dotted lines), and  $-34$  MeV (dashed lines).

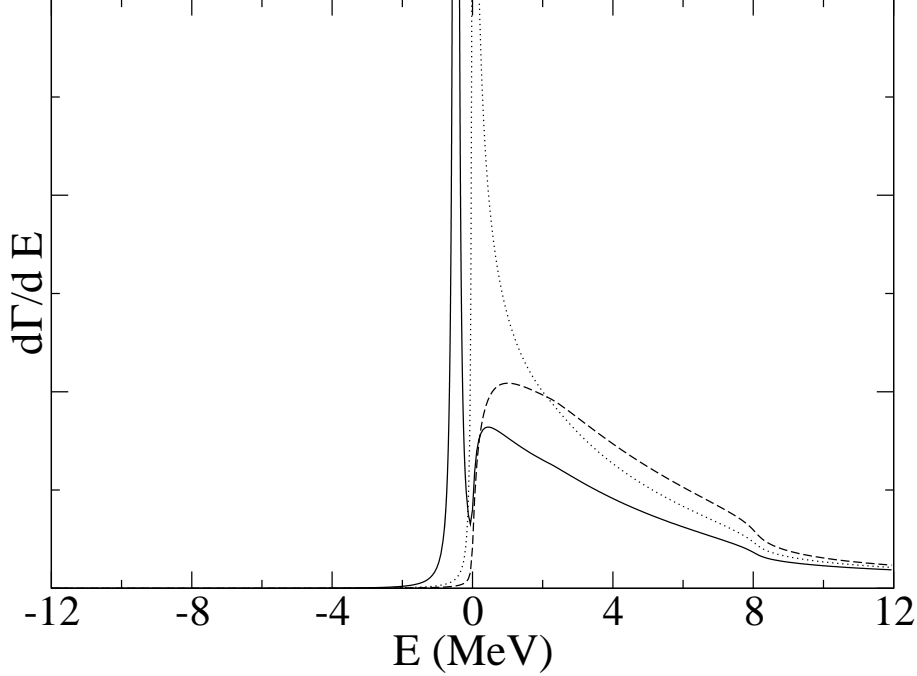


FIG. 6: The line shapes in the  $D^*\bar{D}$  threshold region for  $X(3872)$  produced by a  $B^+ \rightarrow K^+$  or  $B^0 \rightarrow K^0$  transition and decaying into  $D^0\bar{D}^0\pi^0$ . The line shapes are shown for  $\gamma_1 = \pm\infty$  and three values of  $\gamma$ : +34 MeV (solid line), 0 (dotted line), and -34 MeV (dashed line).

approximate zeros near +6 MeV, while the line shapes from the  $B^0 \rightarrow K^+$  transition have approximate zeros near -2 MeV. The relative normalizations of all six curves are determined by using the same short-distance factors  $\Gamma_{B^+}^{K^+,00}$  and  $\Gamma_{J/\psi}^{\pi^+\pi^-}$ . In Fig. 6, we show the line shapes in  $D^0\bar{D}^0\pi^0$ . The line shapes, which are the same for  $X$  produced by a  $B^+ \rightarrow K^+$  or  $B^0 \rightarrow K^0$  transition, are given in Eqs. (79). The relative normalizations of the curves for the three values of  $\gamma$  are determined by using the same short-distance factor  $\Gamma_{B^+}^{K^+,00}$ .

Fig. 5 illustrates the fact that the line shape of the  $X(3872)$  may depend not only on the decay channel but also on the production mechanism for the resonance. The difference between the line shapes in the  $J/\psi\pi^+\pi^-$  decay channel for  $X$  produced by  $B^+ \rightarrow K^+$  and  $B^0 \rightarrow K^0$  transitions is particularly dramatic because of the approximate zeros in the line shapes. These approximate zeros are general features of the line shapes in Eqs. (78). If the imaginary parts of  $\gamma_0$  and  $\kappa_1(E)$  are neglected, the numerator factor  $|\gamma_0 - \kappa_1(E)|^2$  in the energy distribution in Eq. (78a) has a zero between the  $D^{*0}\bar{D}^0$  and  $D^{*+}D^-$  thresholds. If  $|\gamma| \ll |\kappa_1(0)| \ll |\gamma_1|$ , the approximate expression for  $\gamma_0$  in Eq. (34) reduces to  $\kappa_1(0)/2$ . The zero is therefore near  $\frac{3}{4}\nu \approx 6.1$  MeV. If the imaginary parts of  $\gamma_0$  and  $\kappa(E)$  are neglected, the numerator factor  $|\gamma_0 - \kappa(E)|^2$  in the energy distribution in Eq. (78b) has a zero below the  $D^{*0}\bar{D}^0$  threshold. If  $|\gamma| \ll |\kappa_1(0)| \ll |\gamma_1|$ , the zero is near  $-\frac{1}{4}\nu \approx -2.0$  MeV. In the case of  $B^+$  decays, the approximate zero forces the line shape to be narrower on the trailing edge of the resonance. In the case of  $B^0$  decays, the approximate zero forces the line shape to be narrower on the leading edge of the resonance.

In Ref. [19], Braaten and Kusunoki predicted that the decay rate for  $B^0 \rightarrow K^0 + X(3872)$  should be suppressed relative to that for  $B^+ \rightarrow K^+ + X(3872)$ . Their prediction was based on the current-current factorization approximation and heavy-quark symmetry. Together they

imply that, in the  $D^*\bar{D}$  threshold region, the  $B^+ \rightarrow K^+$  transition creates charm mesons predominantly in the neutral channel  $(D^*\bar{D})_+^0$ , while the  $B^0 \rightarrow K^0$  transition creates them predominantly in the charged channel  $(D^*\bar{D})_+^1$ . Since the  $X(3872)$  is a resonance in the  $(D^*\bar{D})_+^0$  channel, the authors of Ref. [19] concluded that the rate for  $B^0 \rightarrow K^0 + X$  must be suppressed relative to that for  $B^+ \rightarrow K^+ + X$ . In retrospect, this prediction was the result of a conceptual error.

The conclusion of Ref. [19] that  $B^0 \rightarrow K^0 + X$  is suppressed follows from the factorization formulas in Sections IV B if  $\kappa_1(0)$  is assumed to be much greater than  $\gamma_0$  and  $\gamma_1$ . In this limit, the two-channel factorization formulas for  $B^+$  decays in Eqs. (77a), (78a), and (79a) all reduce to the single-channel factorization formulas in Eqs. (54) and (55), where  $f(E)$  is the single-channel scattering amplitude in Eq. (14),  $\gamma = (\gamma_1 + \gamma_0)/2$ ,  $\Gamma(E) = 2\Gamma_I(E)$ , and  $\Gamma_{B^+}^{K^+,00} = \Gamma_{B^+}^{K^+,00}$ . For the inverse scattering length  $\gamma$  to be small compared to  $\gamma_0$  and  $\gamma_1$ ,  $\gamma_0$  and  $\gamma_1$  must be nearly equal in magnitude but opposite in sign. If  $\gamma$  is small compared to  $\gamma_1$ , the factorization formula for  $B^0$  decays in Eqs. (77b), (78b), and (79b) also reduce to the single-channel factorization formulas in Eqs. (54) and (55), with  $\Gamma_{B^0}^{K^0} = [\gamma_1/\kappa_1(0)]^2 \Gamma_{B^+}^{K^+}$ . The rate for  $B^0 \rightarrow K^0 + X$  is therefore suppressed by a factor of  $[\gamma_1/\kappa_1(0)]^2$  compared to the rate for  $B^+ \rightarrow K^+ + X$ . Thus the conclusion of Ref. [19] is consistent with the factorization formulas only if the parameters satisfy the hierarchy  $|\gamma| \ll |\gamma_1| \ll |\kappa_1(0)|$ . Since the conclusion of Ref. [19] is only valid in one corner of the parameter space, the authors must have made a conceptual error.

The conceptual error in Ref. [19] has to do with the momentum scale at which the inferences from the current-current factorization approximation and heavy-quark symmetry are applied. Heavy quark symmetry is relevant at energy scales that are small compared to the heavy quark mass  $m_c$  and large compared to the energy scale set by isospin symmetry violations, which is  $\nu \approx 8.1$  MeV. Equivalently, it is relevant at momentum scales that are small compared to  $m_c$  and large compared to  $\kappa_1(0) \approx 125$  MeV. The current-current factorization approximation and heavy quark symmetry imply that the short-distance constant  $\Gamma_{B^+}^{K^+,00} = \Gamma_{B^0}^{K^0,11}$  dominates. This inference should be applied at a momentum scale where heavy quark symmetry applies, which requires the momentum to be large compared to  $\kappa_1(0) \approx 125$  MeV. The conceptual error in Ref. [19] was inferring that the transitions  $B^+ \rightarrow K^+ + (D^*\bar{D})_+^0$  and  $B^0 \rightarrow K^0 + (D^*\bar{D})_+^1$  dominate at a momentum scale small compared to  $\kappa_1(0)$ . At this low momentum scale, there is a resonance only in the  $(D^*\bar{D})_+^0$  channel. However the dominance of  $\Gamma_{B^+}^{K^+,00} = \Gamma_{B^0}^{K^0,11}$  at a scale large compared to  $\kappa_1(0)$  does not imply the dominance of the transitions  $B^+ \rightarrow K^+ + (D^*\bar{D})_+^0$  and  $B^0 \rightarrow K^0 + (D^*\bar{D})_+^1$  at lower scales. As the momentum scale is lowered, resonant scattering between the  $(D^*\bar{D})_+^0$  and  $(D^*\bar{D})_+^1$  channels can feed the transitions  $B^+ \rightarrow K^+ + (D^*\bar{D})_+^1$  and  $B^0 \rightarrow K^0 + (D^*\bar{D})_+^0$ .

To deduce the correct implications of the current-current factorization approximation and heavy quark symmetry at momentum scales small compared to  $\kappa_1(0)$ , we can consider the general factorization formulas in Eqs. (77), (78), and (79) in the low energy region where  $\kappa(E)$  is small compared to  $\kappa_1(0)$ . In this region, the factorization formulas reduce to the single-channel factorization formulas in Eqs. (54) and (55). The assumption that  $\Gamma_{B^+}^{K^+,00} = \Gamma_{B^0}^{K^0,11}$  dominates implies that the short-distance constants for the  $B \rightarrow K$  transition are  $\Gamma_{B^+}^{K^+} \approx \Gamma_{B^+}^{K^+,00}$  and  $\Gamma_{B^0}^{K^0} \approx \Gamma_{B^+}^{K^+,00} |c_1|^2$ , where the coefficient  $c_1$  is given in Eq. (39b). The ratio of the rates is  $|c_1|^2 = |\gamma_1|^2/|\gamma_1 - \kappa_1(0)|^2$ . If we ignore the small imaginary parts of  $\gamma_1$  and  $\kappa_1(0)$ , this ratio is greater than 1 if  $\gamma_1 > \kappa_1(0)/2$  and less than 1 if  $\gamma_1 < \kappa_1(0)/2$ . Thus the rate for  $B^0 \rightarrow K^0 + X$  need not be suppressed compared to that for  $B^+ \rightarrow K^+ + X$ .

## V. SUMMARY

In Ref. [26], we derived line shapes of the  $X(3872)$  that should be accurate in the region within a few MeV of the  $D^{*0}\bar{D}^0$  threshold. The line shapes were derived from an expression for the resonant scattering amplitude in the  $(D^*\bar{D})_+^0$  channel that takes into account the  $D^{*0}$  width and inelastic charm meson scattering channels. In the factorization formulas for the line shapes, short-distance effects and long-distance effects are separated into multiplicative factors. The line shapes of Ref. [26] are independent of the production mechanism for the  $X$  resonance. The line shape in  $D^0\bar{D}^0\pi^0$  is different from the line shape in a short-distance decay mode, such as  $J/\psi\pi^+\pi^-\pi^0$  or  $J/\psi\pi^+\pi^-$ . As shown by the analysis of Ref. [26], the difference in these line shape can explain the difference between the masses of  $X(3872)$  measured in the  $J/\psi\pi^+\pi^-$  and  $D^0\bar{D}^0\pi^0$  decay modes [6, 7].

In this paper, we have derived line shapes for the  $X(3872)$  whose region of validity extends to the entire  $D^*\bar{D}$  threshold region by taking into account the resonant coupling between the  $(D^*\bar{D})_+^0$  and  $(D^*\bar{D})_+^1$  channels. By taking into account isospin symmetry at high energies, the coupled-channel scattering amplitudes were expressed in terms of two parameters: the  $I = 0$  and  $I = 1$  inverse scattering amplitudes  $\gamma_0$  and  $\gamma_1$ . Isospin symmetry was also taken into account in the short-distance factors in the factorization formulas. In the case of production of the  $X$  resonance in  $B \rightarrow K$  transitions, isospin symmetry reduces the short-distance factors to four independent real constants:  $\Gamma_{B^+}^{K^+,00}$ ,  $\Gamma_{B^+}^{K^+,11}$ , and the real and imaginary parts of  $\Gamma_{B^+}^{K^+,01}$ . The resulting factorization formulas for the inclusive resonance production rate in the  $B^+ \rightarrow K^+$  transition is given in Eq. (57). The factorization formula for the  $D^0\bar{D}^0\pi^0$  channel is given in Eq. (62). The factorization formulas for  $I = 0$  and  $I = 1$  short-distance decay channels are given for both the  $B^+ \rightarrow K^+$  and the  $B^0 \rightarrow K^0$  transitions in Eqs. (72) and (73). The line shape in an  $I = 0$  short-distance decay channel, such as  $J/\psi\pi^+\pi^-\pi^0$ , is different from the line shape in an  $I = 1$  short-distance decay channel, such as  $J/\psi\pi^+\pi^-$ . The line shapes for the  $X$  resonance produced by the  $B^+ \rightarrow K^+$  transition are also different from the line shapes produced by the  $B^0 \rightarrow K^0$  transition.

If we use the current-current factorization approximation together with heavy quark symmetry, the factorization formulas simplify dramatically. The factorization formulas for an  $I = 0$  decay channel, an  $I = 1$  decay channel, and  $D^0\bar{D}^0\pi^0$  are given in Eqs. (77), (78), and (79), respectively. The short-distance constants associated with the  $B \rightarrow K$  transitions reduce to a single real constant  $\Gamma_{B^+}^{K^+,00}$ . Thus the ratios of production rate in  $B^+ \rightarrow K^+$  transitions and in  $B^0 \rightarrow K^0$  transitions are completely determined by the scattering parameters  $\gamma_0$  and  $\gamma_1$ .

Our results allow us to identify conceptual errors in previous work on this problem. In Ref. [19], Braaten and Kusunoki predicted that  $B^0 \rightarrow K^0 + X$  should be suppressed by at least an order of magnitude compared to  $B^+ \rightarrow K^+ + X$ . The prediction was based on the current-current approximation and heavy quark symmetry. The conceptual error was an implicit assumption that  $\gamma_0$  and  $\gamma_1$  are small compared to  $\kappa_1(0)$ . In Ref. [29], Voloshin predicted that the line shapes for the  $X$  resonance produced by  $B^+ \rightarrow K^+ + X$  and  $B^0 \rightarrow K^0 + X$  should be identical. The conceptual errors were ignoring resonant scattering between the  $(D^*\bar{D})_+^0$  and  $(D^*\bar{D})_+^1$  channels and failing to take into account isospin symmetry in the  $B \rightarrow K$  transitions.

Our results provide a physical interpretation for the model of the  $(D^*\bar{D})_+^0$  scattering amplitude used in Ref. [25]. The scaling behavior of the fits in Ref. [25] indicate that the term  $-(2/g)E$  in the inverse of the scattering amplitude in Eq. (43) can be omitted. The

resulting scattering amplitude is essentially equivalent to the general  $(D^*\bar{D})_+^0$  scattering amplitude  $f_{00}(E)$  in Eq. (29a) in the limit  $|\gamma_1| \gg |\kappa_1(0)|$ .

The most important parameters for predicting the line shapes are the scattering parameters  $\gamma_0$  and  $\gamma_1$ . They could be determined phenomenologically from ratios of rates for  $B^0 \rightarrow K^0 + X$  and  $B^+ \rightarrow K^+ + X$ . Alternatively they could be calculated using the meson potential model of Ref. [27]. If these scattering parameters were calculated, the predictive power of the results of this paper would be dramatically increased. The line shapes for the  $X(3872)$  resonance produced by  $B \rightarrow K$  transitions also depend on the short-distance factors  $\Gamma_{B^+}^{K^+,00}$ ,  $\Gamma_{B^+}^{K^+,01}$ , and  $\Gamma_{B^+}^{K^+,11}$ . They could be determined phenomenologically from measurements of the charm meson invariant mass distributions in the decays  $B \rightarrow K + D^*\bar{D}$  and  $B \rightarrow K + D\bar{D}^*$ .

The accuracy of our predictions for the line shapes could be further improved by taking into account pions explicitly. The system consisting of  $D^{*0}\bar{D}^0$ ,  $D^0\bar{D}^{*0}$ , and  $D^0\bar{D}^0\pi^0$  states with energies near the  $D^0\bar{D}^{*0}$  threshold can be described by a nonrelativistic effective field theory. The simplest such theory has S-wave scattering in the  $(D^*\bar{D})_+^0$  channel and  $\pi^0$  couplings that allow the decay  $D^{*0} \rightarrow D^0\pi^0$ . Fleming, Kusunoki, Mehen, and van Kolck developed power-counting rules for this effective field theory and showed that the pion couplings can be treated perturbatively [30]. They used the effective field theory to calculate the decay rate for  $X(3872) \rightarrow D^0\bar{D}^0\pi^0$  to next-to-leading order in the pion coupling. In applying this effective field theory to the line shapes of the  $X(3872)$ , one complication that will be encountered is infrared singularities at the  $D^{*0}\bar{D}^0$  threshold that are related to the decay  $D^{*0} \rightarrow D^0\pi^0$ . This problem has been analyzed in a simpler model with spin-0 particles and momentum-independent interactions [31]. The problem was solved by a resummation of perturbation theory that takes into account the perturbative shift of the  $D^0\bar{D}^{*0}$  threshold into the complex energy plane because of the nonzero width of the  $D^{*0}$ .

In summary, the establishment of the quantum numbers of the  $X(3872)$  as  $1^{++}$  and the measurement of its mass imply that it is either a charm meson molecule or a charm meson virtual state. These two possibilities can be distinguished in practice by their different predictions for the line shapes of the  $X(3872)$ . The analysis of Ref. [26] indicates that the existing data favor a charm meson molecule, but a virtual state is not excluded. The expressions for the line shapes used in that analysis should be accurate only within a few MeV of the  $D^{*0}\bar{D}^0$  threshold. The expressions for the line shapes derived in this paper should be accurate in the entire  $D^*\bar{D}$  threshold region. When more extensive data on the line shapes of the  $X(3872)$  in various decay channels and for various production processes becomes available, it should be possible to determine conclusively whether the  $X(3872)$  is a bound state or a virtual state of charm mesons.

## Acknowledgments

This research was supported in part by the Department of Energy under grant DE-FG02-91-ER40690.

---

[1] S. K. Choi *et al.* [Belle Collaboration], “Observation of a new narrow charmonium state in exclusive  $B^+ \rightarrow \text{Phys. Rev. Lett. } \mathbf{91}, 262001$  (2003) [arXiv:hep-ex/0309032].

- [2] D. Acosta *et al.* [CDF II Collaboration], Phys. Rev. Lett. **93**, 072001 (2004) [arXiv:hep-ex/0312021].
- [3] V. M. Abazov *et al.* [D0 Collaboration], Phys. Rev. Lett. **93**, 162002 (2004) [arXiv:hep-ex/0405004].
- [4] B. Aubert *et al.* [BABAR Collaboration], Phys. Rev. D **71**, 071103 (2005) [arXiv:hep-ex/0406022].
- [5] K. Abe *et al.*, arXiv:hep-ex/0505037.
- [6] G. Gokhroo *et al.*, Phys. Rev. Lett. **97**, 162002 (2006) [arXiv:hep-ex/0606055].
- [7] B. Aubert *et al.* [BABAR Collaboration], arXiv:0708.1565 [hep-ex].
- [8] K. Abe *et al.* [Belle Collaboration], arXiv:hep-ex/0505038.
- [9] A. Abulencia *et al.* [CDF Collaboration], Phys. Rev. Lett. **96**, 102002 (2006) [arXiv:hep-ex/0512074].
- [10] W. M. Yao *et al.* [Particle Data Group], J. Phys. G **33**, 1 (2006).
- [11] C. Cawfield *et al.* [CLEO Collaboration], Phys. Rev. Lett. **98**, 092002 (2007) [arXiv:hep-ex/0701016].
- [12] N. A. Tornqvist, Phys. Lett. B **590**, 209 (2004) [arXiv:hep-ph/0402237].
- [13] F. E. Close and P. R. Page, Phys. Lett. B **578**, 119 (2004) [arXiv:hep-ph/0309253].
- [14] S. Pakvasa and M. Suzuki, Phys. Lett. B **579**, 67 (2004) [arXiv:hep-ph/0309294].
- [15] M. B. Voloshin, Phys. Lett. B **579**, 316 (2004) [arXiv:hep-ph/0309307].
- [16] E. Braaten and H. W. Hammer, Phys. Rept. **428**, 259 (2006) [arXiv:cond-mat/0410417].
- [17] E. Braaten and M. Kusunoki, Phys. Rev. D **69**, 074005 (2004) [arXiv:hep-ph/0311147].
- [18] E. Braaten, M. Kusunoki and S. Nussinov, Phys. Rev. Lett. **93**, 162001 (2004) [arXiv:hep-ph/0404161].
- [19] E. Braaten and M. Kusunoki, Phys. Rev. D **71**, 074005 (2005) [arXiv:hep-ph/0412268].
- [20] E. Braaten and M. Kusunoki, Phys. Rev. D **72**, 014012 (2005) [arXiv:hep-ph/0506087].
- [21] E. Braaten and M. Kusunoki, Phys. Rev. D **72**, 054022 (2005) [arXiv:hep-ph/0507163].
- [22] E. Braaten and M. Lu, Phys. Rev. D **74**, 054020 (2006) [arXiv:hep-ph/0606115].
- [23] E. S. Swanson, Phys. Rept. **429**, 243 (2006) [arXiv:hep-ph/0601110].
- [24] D. V. Bugg, Phys. Lett. B **598**, 8 (2004) [arXiv:hep-ph/0406293].
- [25] C. Hanhart, Yu. S. Kalashnikova, A. E. Kudryavtsev and A. V. Nefediev, Phys. Rev. D **76**, 034007 (2007) [arXiv:0704.0605 [hep-ph]].
- [26] E. Braaten and M. Lu, arXiv:0709.2697 [hep-ph].
- [27] N. A. Tornqvist, Z. Phys. C **61**, 525 (1994) [arXiv:hep-ph/9310247].
- [28] S. Flatté, Phys. Lett. **63B**, 224 (1976).
- [29] M. B. Voloshin, Phys. Rev. D **76**, 014007 (2007) [arXiv:0704.3029 [hep-ph]].
- [30] S. Fleming, M. Kusunoki, T. Mehen and U. van Kolck, Phys. Rev. D **76**, 034006 (2007) [arXiv:hep-ph/0703168].
- [31] E. Braaten, M. Lu and J. Lee, Phys. Rev. D **76**, 054010 (2007) [arXiv:hep-ph/0702128].